

1 **Quantifying Workers' Gait Patterns to Identify Safety Hazards in Construction Using a Wearable**
2 **Insole Pressure System**

3
4 Maxwell Fordjour Antwi-Afari^{1*}, Heng Li², Shah Nawaz Anwer³, Sitsofe Kwame Yevu⁴, Zezhou Wu⁵,
5 Prince Antwi-Afari⁶, Inhan Kim⁷

6 ¹Postdoctoral Research Fellow, Department of Building and Real Estate, Faculty of Construction and
7 Environment, Hong Kong Polytechnic University, Room No. ZN1002, Hung Hom, Kowloon, Hong
8 Kong Special Administrative Region, E-mail: maxwell.antwifari@connect.polyu.hk

9
10 ²Chair Professor, Department of Building and Real Estate, Faculty of Construction and Environment, Hong
11 Kong Polytechnic University, Room No. ZS734, Hung Hom, Kowloon, Hong Kong Special Administrative
12 Region, E-mail: heng.li@polyu.edu.hk

13
14 ³PhD Candidate, Department of Building and Real Estate, Faculty of Construction and Environment, Hong
15 Kong Polytechnic University, Room No. ZN1002, Hung Hom, Kowloon, Hong Kong Special Administrative
16 Region, E-mail: shahnawaz.anwer@connect.polyu.hk

17
18 ⁴PhD Candidate, Department of Building and Real Estate, Faculty of Construction and Environment, Hong
19 Kong Polytechnic University, Room No. ZN712, Hung Hom, Kowloon, Hong Kong Special Administrative
20 Region, E-mail: sitsofe-k.yevu@connect.polyu.hk

21
22 ⁵Assistant Professor, Department of Construction Management and Real Estate, College of Civil and
23 Transportation Engineering, Shenzhen University, Shenzhen 518000, China, E-mail: wuzezhou@szu.edu.cn

24
25 ⁶PhD Student, Department of Civil Engineering, Faculty of Engineering, The University of Hong Kong,
26 Pokfulam, Hong Kong Special Administrative Region, E-mail: pantwif@connect.hku.hk

27
28 ⁷Professor, Department of Architecture, KyungHee University, Seoul, South Korea, E-
29 mail: ihkim1@gmail.com

30
31
32 ***Corresponding author:**
33 Dr Maxwell Fordjour Antwi-Afari
34 E-mail: maxwell.antwifari@connect.polyu.hk

35
36
37

38 **Highlights**

- 39 • A safety hazard identification approach based on gait disruption patterns is
40 proposed.
- 41 • Gait variability parameters were measured from a wearable insole pressure system.
- 42 • A strong correlation between gait abnormalities and a safety hazard location is
43 found.
- 44 • The proposed approach could help to mitigate non-fatal fall injuries in construction.

45 **1. Introduction**

46 The construction industry is highly regarded as a labour-intensive and hazardous occupation. Compared to
47 other industries, the construction industry has achieved the highest number of occupational fatal and non-
48 fatal injuries (International Labor Organization, 2016). In the United States, more than 700 fatal and 200,000
49 non-fatal injuries are reported every year (Bureau of Labor Statistics (BLS), 2017). In Australia, there were
50 35 out of 182 fatalities in the construction industry in 2016, which accounted for 3.3 fatality rate (fatalities
51 per 100,000 workers) across all industries (Safe Work Australia, 2017). These occupational injuries can lead
52 to substantial disorders, project delays, increased project costs, workers absenteeism, medical burden and
53 permanent disabilities (Antwi-Afari et al., 2017b; Umer et al., 2017a; Antwi-Afari et al., 2018a; Kong et al.,
54 2018). To tackle the menace of occupational injuries in construction, researchers and practitioners have to
55 focus on identifying safety hazards and suggesting proactive injury-prevention measures.

56

57 Safety hazard identification is a fundamental approach for improving construction safety management,
58 especially when assessing non-fatal fall injuries. Slips, trips, and unexpected step-down hazards are
59 recognized as the primary initiating hazards that may lead to non-fatal fall injuries among construction
60 workers (Yoon and Lockhart, 2006; Antwi-Afari et al., 2018e). To prevent the occurrence of these safety
61 hazards, the construction industry has adopted a number of traditional safety hazards identification methods
62 such as job-hazard analyses, pre-task safety meetings, safety checklists, and safety training (Rozenfeld et al.,
63 2010; Albert et al., 2014b). Despite their usefulness, there are few limitations of the aforementioned methods
64 which had led to poor safety hazard identification performance. Examples of these limitations include (1)
65 limited availability of resources (e.g., safety inspectors) to assess multiple areas (Albert et al., 2014b); (2)
66 different levels of knowledge, experience, judgments or techniques (e.g., past accident cases or regulations)
67 for identifying hazards (Albert et al., 2014a); (3) unable to continuously identify hazards due to decrease
68 individual's ability and a dynamic construction environment (Park et al., 2016). Given above, many safety
69 hazards remain unidentified or not well assessed, which may expose construction workers to a high risk of
70 developing non-fatal fall injuries (Carter and Smith, 2006; Albert et al., 2014b). To address the limitations
71 of current methods and prevent non-fatal fall injuries, different approaches have been tested to identify safety
72 hazards in construction.

73

74 Recently, one of the potential approaches for identifying safety hazards in construction relied on collecting
75 workers' bodily or gait responses by using wearable inertial measurement units (WIMUs) system. In the
76 realm of construction, previous studies have demonstrated the feasibility of using WIMU-based systems for
77 identifying safety hazards (Akhavian and Behzadan, 2016; Jebelli et al., 2016a; Kim et al., 2016; Yang et al.,
78 2017). The findings of these studies revealed that workers' gait patterns contain a valuable source of
79 information for identifying different types of safety hazards in both laboratory and construction site settings
80 without relying on experts' judgment. Despite its usefulness, this approach requires multiple WIMU based-
81 systems to be attached to workers' body (e.g., ankle, waist) to mainly collect acceleration or kinematic gait
82 responses for identifying safety hazards. As a result, attaching multiple WIMU-based systems to the skin
83 surfaces may not only lead to workers' discomforts and inconveniences but also may reduce construction
84 workers' productivity (Antwi-Afari and Li, 2018g; Antwi-Afari et al., 2019c). In addition, WIMU-based
85 systems are difficult to acquire ground reaction force (GRF) data when workers use their feet as the main
86 support of the whole body (Antwi-Afari et al., 2018f). Moreover, they are intrusive and normally require
87 indirect forms of attachments such as straps, belts, or other accessories to prevent detachment of sensors from
88 the body when performing a given task. Consequently, there is a critical need to propose a non-invasive
89 approach that would enhance safety hazard identification methods to prevent non-fatal fall injuries on a
90 construction site.

91
92 Therefore, this research proposes a novel and non-invasive approach to examine the feasibility of using
93 workers' gait disruption patterns captured by a wearable insole pressure system to identify safety hazards
94 among construction workers. It was hypothesized that workers' gait disruption patterns quantified as either
95 gait variability parameters or gait abnormality based on GRF deviation in a specific location has a strong
96 relationship with the presence of a hazard in that location. To test this hypothesis, this study was conducted
97 in a laboratory setting to examine and compare gait abnormality measurements during a normal gait (i.e., no
98 [hazard condition](#)) to three different hazard conditions such as a [slippery surface hazard](#), [an obstacle hazard](#),
99 [and an uneven surface hazard](#). The main contribution of this study attempts to use a wearable sensing
100 technique (i.e., a non-invasive wearable insole pressure system) for continuous monitoring and identification
101 of safety hazards in a timely manner. The proposed approach could serve as a piece of personal protective

102 equipment to help researchers and safety managers to identify workers' exposure to safety hazards and also
103 extends the current wearable sensing technologies for construction safety research.

104

105 **2. Research background**

106 *2.1. Methods for identifying safety hazards in construction*

107 To successfully mitigate non-fatal fall injuries among construction workers, researchers and safety managers
108 need to adopt a novel method for identifying safety hazards on construction sites. There are already existing
109 safety hazard identification methods that are applied in the construction industry. Examples of these methods
110 include (1) predictive methods such as job-hazard analyses, pre-task safety meetings (Rozenfeld et al., 2010;
111 Mitropoulos and Namboodiri, 2011); and (2) retrospective methods such safety checklists (Chi et al., 2005;
112 Goh and Chua, 2009). Taken together, these existing methods require construction workers to either predict
113 expected safety hazards or learned lessons from past safety incidents to prevent the occurrence of future
114 safety hazards. Despite their usefulness, they perform poorly because of the following limitations: 1)
115 individual workers do not share the same level of knowledge and experience in regard to identifying hazard
116 conditions; 2) very time-consuming and error-prone due to the dynamic and unpredicted nature of
117 construction environment which makes hazard recognition more challenging.

118

119 In addition, previous studies on safety hazard identification have explored other existing methods such as
120 training programs or training in virtual environments (Kaskutas et al., 2013; Albert et al., 2014a, Albert et
121 al., 2014b). Kaskutas et al. (2013) studied the effect of training on residential foremen and showed that
122 training can enhance workers' exposure to safety hazards and improve safety behaviours at worksites. Despite
123 advances in safety training, safety hazard identification is mostly performed manually by construction
124 workers or safety managers. Consequently, construction sites still have many unidentified hazards, and the
125 risk of non-fatal fall injuries remains high (Albert et al., 2014a).

126

127 To overcome existing methods, a number of advanced sensing approaches (Antwi-Afari et al., 2019a) have
128 been proposed for identifying safety hazards. Several studies examined the potential of applying computer
129 vision-based techniques (e.g., depth sensors or stereo camera) to automatically detect safety hazards in

130 construction (Han et al., 2012; Weerasinghe et al., 2012; Han and Lee, 2013). However, the application of
131 vision-based techniques has several challenges, including the limited sensing range of a camera, visual
132 occlusions and misrepresentation. In addition, they require a direct line of sight is to register human
133 movements (Valero et al., 2017). Other researchers have demonstrated different sensing approaches such as
134 radio frequency identification (RFID) (Teizer et al., 2010, Lee et al., 2011), Bluetooth sensing technology
135 (Park et al., 2015), building information modeling (Qi et al., 2013), case-based reasoning (Goh and Chua,
136 2009), a global positioning system (GPS) (Wang and Razavi, 2016) and virtual reality approaches (Albert et
137 al., 2014a). Most of these sensing approaches have verified the capabilities of mitigating the proximity of
138 safety hazards on construction sites, especially from severe injuries resulting from workers being struck by
139 vehicles or equipment (Teizer et al., 2010; Park et al., 2015; Wang and Razavi, 2016). Although useful, these
140 sensing approaches have not become mainstream within the construction industry for safety hazard
141 identification. Besides, they mostly rely on pre-defined sets of hazard information (e.g., regulations,
142 standards, specifications) and are unable to identify undefined safety hazards (e.g., slips, trips) associated
143 with unsafe surface conditions. Moreover, these sensing approaches enable workers or safety managers to
144 still apply manual observation to identify hazards, which can be difficult to identify safety hazards due to the
145 dynamic and unique construction environment. Therefore, to prevent non-fatal fall injuries, a novel method
146 for identifying safety hazard is still necessary.

147

148 With the development of wearable sensing technologies, previous studies have extensively demonstrated the
149 use of WIMU-based systems to identify safety hazards (Jebelli et al., 2016a; Kim et al., 2016; Yang et al.,
150 2017; Kim et al., 2018). In clinical and rehabilitation settings, previous researches have widely used WIMU-
151 based systems for continuous and objective identification of safety hazards (Culhane et al., 2005; Boyle et
152 al., 2006; Howcroft et al., 2013). In the realm of construction, Dzung et al. (2014) investigated whether it
153 was possible to detect fall portents—i.e., near-miss falls—using embedded WIMU sensors in a smartphone.
154 Jebelli et al. (2016a) examined the usefulness of gait-stability metric—which are computed by using collected
155 data from WIMUs—in differentiating high-fall-risk tasks of ironworkers. Kim et al. (2016) examined the
156 feasibility of using WIMU-based systems to analyze how workers' bodily responses could allow for the
157 identification of a safety hazard on a construction job site. Yang et al. (2017) proposed a collective sensing

158 approach by using WIMU-based systems to assess workers' gait abnormalities to identify safety hazards in
159 construction. Overall, these studies have established the feasibility of using WIMU-based systems to capture
160 workers' abnormal gait patterns and/or bodily responses for identifying potential safety hazards. In addition,
161 they have shown that WIMU-based systems provide relatively objective and continuous data in construction
162 environments conditions when compared to the traditional methods.

163

164 There are some limitations for identifying safety hazards by using WIMU-based systems. First, it can capture
165 thresholds such as the magnitude of angular velocity and acceleration signals as the main source of data to
166 detect different types of safety hazards when observing bodily responses or gait patterns. However, such
167 thresholds diminish the automation potential of these approaches (Yang and Ahn, 2019). Second, they require
168 the use of multiple WIMU-based systems to be attached to the subject's lower body parts (e.g., ankle) for
169 ambulatory gait analysis (Antwi-Afari, 2019). Despite being non-intrusive, attaching WIMU-based systems
170 to the skin surfaces may not only lead to workers' discomforts and inconveniences but also may reduce
171 construction workers' productivity (Antwi-Afari et al., 2018c; Antwi-Afari et al., 2019c). Third, the results
172 of previous studies indicated that such approaches required a large amount of sensed data to reliably estimate
173 hazard locations, as bodily responses do not contain direct information about the interaction between a
174 worker's foot and the surface conditions on a job site (Kim et al., 2016; Yang et al., 2017). Given the above
175 limitations, a novel approach that can resolve current limitations is necessary to enhance safety hazard
176 identification on construction sites.

177

178 To address these knowledge gaps, the current study proposes a novel and non-invasive approach to examine
179 the feasibility of using workers' gait disruption patterns captured by a wearable insole pressure system to
180 identify safety hazards among construction workers. Different from previous studies, the present study used
181 spatiotemporal gait features and gait abnormality based on GRF deviation to quantify the workers' gait
182 disruption patterns in order to identify safety hazards on construction sites. As such, the proposed approach
183 might not only collect foot plantar pressure patterns and GRF data between a worker's foot and the unsafe
184 surface conditions but also provides less constraint in workers' bodily movements.

185

186 2.2. *Gait abnormality measurements to identify safety hazards—the feasibility of using gait disruption*
187 *patterns measured by a wearable insole pressure system*

188 Falls are the main contributing cause of fatal injuries and the third leading cause of non-fatal injuries in
189 construction (CPWR, 2013). According to the BLS in the United States, falls injuries accounted for
190 approximately 30% of all fatalities in construction (BLS, 2015). In 2017, the Development Bureau in Hong
191 Kong reported that non-fatal fall injuries such as slip, trip, and other loss of balance **hazards** are the most
192 common types of accidents, which accounted for 19.8% of the total number of accidents (Development
193 Bureau, 2017). Consequently, many studies have provided valuable insights into the prevalent of fall injuries
194 on construction sites (Dong et al., 2009; Wong et al., 2016). Dong et al. (2009) evaluated fall injuries among
195 Hispanic construction workers; and found that about every two or three fatal falls in construction occurred in
196 the establishment with 10 or fewer workers. Wong et al. (2016) investigated the root causes of falls from
197 height, finding that workers' loss of balance and not wearing fall protection devices account for 48% of fall
198 injuries in Hong Kong. Chi et al. (2005) identified contributing factors to fatal fall accidents in construction
199 and suggested prevention measures for fall accidents. Although these previous studies **offer** insights on the
200 prevalence and how to mitigate the risk of fatal and non-fatal fall injuries, safety hazard identification is
201 arguably the most fundamental element of any safety management program to prevent non-fatal fall injuries
202 in construction.

203
204 Regardless of the extensive research, safety hazard identification is the critical first step in construction safety
205 management to mitigate **safety hazards (e.g., slip, trip, unexpected step-down)** that may lead workers to
206 develop non-fatal fall injuries (Carter and Smith, 2006). Previous studies have proposed the evaluation of
207 workers' abnormal gait patterns (Yoon and Lockhart, 2006; Yang et al., 2017; Yang et al., 2019), losing
208 balance events (Yang et al., 2016), the magnitude of bodily responses (Kim et al., 2016), and trajectory
209 patterns (Yang et al., 2018) measured by WIMU-based systems to identify safety hazards. By considering
210 the different measurement approaches, workers' abnormal gait patterns are particularly useful for identifying
211 safety hazards and assessing the risk of non-fatal fall injuries among construction workers. This is because
212 factors contributing to non-fatal fall injuries are often caused by the interactions between the human feet and
213 unsafe surface conditions such as obstacle, uneven surface, and slippery surface hazards (Decker et al., 2009).

214 Consequently, the changes in workers' abnormal gait patterns might provide a new insight for identifying
215 safety hazard in order to prevent non-fatal fall injuries in construction.

216

217 The feasibility of evaluating gait variability parameters (i.e., spatiotemporal gait features and gait
218 abnormalities) obtained by using a wearable insole pressure system for identifying the existence of safety
219 hazards has been studied in many disciplines such as clinical (Li et al., 2018), sport science (Harle et al.,
220 2012) and rehabilitation settings (Bae et al., 2011; David et al., 2017; Solanki and Lahiri, 2018). Specifically,
221 these applications range from evaluating the efficacy of walking patterns in cerebral palsy (Nsenga Leunkeu
222 et al., 2014), through aiding diagnosis and assessment of neuropathies (David et al., 2017; Solanki and Lahiri,
223 2018) to monitoring gait abnormalities, assessing fall risks and preventing falls for the elderly (Howcroft et
224 al., 2016). Notably, most of the activities performed by patients were mainly to differentiate their daily
225 physical activities such as standing, sitting and walking (David et al., 2017; Li et al., 2018). However,
226 construction workers are frequently exposed to unsafe surface conditions such as obstacle, slippery surface,
227 and uneven surface hazards, and the performance of gait variability parameters measured by using a wearable
228 insole pressure system has not been studied in the construction environments.

229

230 The results of previous studies had confirmed the feasibility of using a wearable insole pressure system to
231 evaluate gait variability parameters (Bae et al., 2011; David et al., 2017; Solanki and Lahiri, 2018). Although
232 these gait variability parameters have been used to evaluate the fall risks of patients, no previous study has
233 utilized gait variability parameters measured by a wearable insole pressure system to identify safety hazards
234 in construction environments. Antwi-Afari and Li (2018g) examined the changes in spatial foot regions and
235 loss of balance events associated with biomechanical gait stability parameters based on foot plantar pressure
236 patterns measured by a wearable insole pressure system. Although our previous results provided useful gait
237 metric, the changes in gait speed and different participants' body weight during data collection may influence
238 the reliability of gait stability parameters. As such, biomechanical gait stability parameters may not be
239 suitable for a dynamic and unique construction environment. Unlike our previous study, this present study
240 computed gait variability parameters by using pressure-sensitive elements and GRF data captured by a
241 wearable insole pressure system to identify safety hazards. However, it is not certain whether each

242 spatiotemporal gait feature is sensitive to a specific type of hazard. Moreover, each gait feature has a different
 243 range of values with different measurement units. Thus, in this current study, to comprehensively assess the
 244 workers' gait abnormalities caused by safety hazards, it is necessary to represent the deviations of gait
 245 features from a normal gait in a single value by using the magnitude of the GRF. Overall, the proposed
 246 approach can help construction managers eliminate the risk of hazards without depending exclusively upon
 247 traditional safety hazard identifications such as manual observations.

248

249 3. Research methods

250 3.1. Participants

251 A convenience sample of ten healthy male volunteers was recruited from the student population of the Hong
 252 Kong Polytechnic University. Table 1 presents the participants' demographic characteristics. All participants
 253 were screened based on a face to face interview and physical examination of their feet or gait abnormalities.
 254 Exclusion criteria were: (1) history of significant foot injuries or lower-extremities abnormalities during the
 255 last 12 months preceding the start of the study; (2) history of neurological conditions or disabilities or other
 256 conditions that affected fall and/or balance. With the approval of the Human Subject Ethics Subcommittee
 257 of the Hong Kong Polytechnic University (reference number: *HSEARS20170605001*), written consent was
 258 obtained from the participants after a verbal and written explanation of the experimental procedures.

259

260 **Table 1.** Participants' demographic characteristics.

Demographic Characteristics	Mean	Median	Standard Deviation	Minimum Value	Maximum Value
Age (years)	31.70	31.50	3.65	26	38
Height (m)	1.62	1.60	0.13	1.40	1.80
Weight (kg)	77.20	77.50	8.40	65	90
Shoe size (European)	42.60	43	0.52	42	43
Foot length (mm)	27.17	27.70	1.38	24.30	28.50
Foot width (mm)	9.61	9.60	0.32	9.20	10.20

261

262 3.2. Experimental apparatus

263 An OpenGo system (Moticon SCIENCE Sensor Insole GmbH, Munich, Germany), which is a wearable
 264 insole pressure system was used for collecting foot plantar pressure distribution and GRF data in this study.

265 Each left or right sensor insole contains 16 capacitive pressure sensors and a 6-axis gyroscope (MEMS
266 LSM6DSL, ST Microelectronics) for acceleration and angular rate data. Pressure sensors have a range,
267 resolution and hysteresis of 0 to 50.0 N/cm², 0.25 N/cm² and ≤ 1%, respectively. Manufacturer’s guidelines
268 indicate that no calibration is needed within its production lifetime. The acceleration range and angular rate
269 range are ± 16g and ± 2000 dps, respectively. The sampling frequency ranges from 10 to 100Hz. Each sensor
270 insole contains on-board memory storage (16 MB) and a coin cell rechargeable of 3.7 V± 0.4V power supply.
271 It uses a Bluetooth low energy 5.0 for wireless transmission within a wireless range of ≥ 5.0m and bandwidth
272 of 54 kB/s. The sensor insoles are available in different sizes, operation modes and provide valuable
273 information regarding a participant’s foot plantar pressure distribution, body weight, balance and motion
274 analysis.

275

276 3.3. *Experimental design and procedure*

277 The current study adopted a randomized crossover study design in a single testing session (Fig. 1). As shown
278 in Fig. 1, the participants were randomly assigned to different randomized trials of experiments. As a result,
279 each participant received different randomized trials during different time periods (Fig. 1). It was revealed
280 that the first randomized experimental trial for “Participant 1” was repeated as the third randomized
281 experimental trial for “Participant 2” and also crossed over as the second randomized experimental trial for
282 “Participant 3” (Fig. 1). The purpose of the adopted study design was to achieve comparable groups of
283 randomized experimental trials while preventing selection bias. Fig. 2 presents the laboratory experiments.
284 As depicted in Fig. 2, a simulated laboratory experiment was conducted to collect participants’ gait disruption
285 patterns when they were exposed to safety hazards. In particular, this study tested three different types of
286 hazards, namely a slippery surface hazard (Fig. 2d), an obstacle hazard (Fig. 2e), and an uneven surface
287 hazard (Fig. 2f). To simulate these hazards in a laboratory as though similar to real construction environment,
288 the participants wore a pair of safety boot, safety harness, and safety helmet during the testing session. In
289 order to prevent unforeseen injuries and reduce the adverse impacts of the experimental trials on the
290 surrounding environment, a safety harness and a 30-cm thick layer of high-density gymnasium mattress were
291 provided during the testing session. The experimenter conducted training sessions for the participants to
292 practice the exposure of each hazard after watching representative videos of real-time occurrences of safety

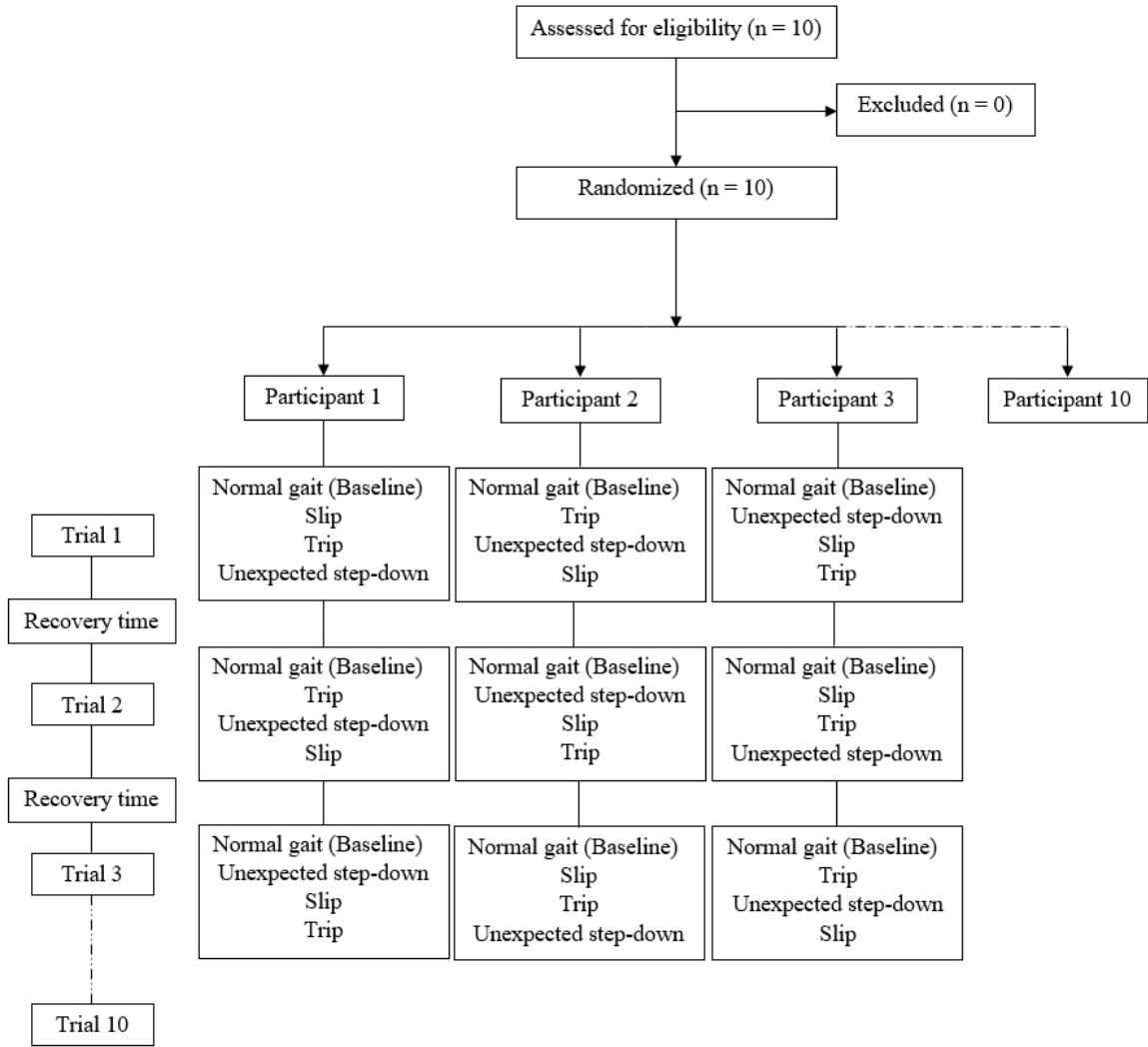
293 hazards on construction sites. The participants were instructed to walk at their comfortable pace along a
294 particular path so that they cannot avoid a hazard on the floor surface.

295

296 In this study, three main safety hazards were tested at a specific location (i.e., 5m) during the laboratory
297 experiments (Fig. 2): (1) a slippery surface hazard (i.e., a low-density polyethylene) that may cause a slip
298 hazard (Fig. 2a); an obstacle hazard (i.e., a concrete brick measuring 20cm × 9cm × 6cm height) that may
299 cause a trip hazard (Fig. 2b); and (3) an uneven surface hazard (i.e., a wooden platform with 20 cm height)
300 that may cause an unexpected step-down hazard (Fig. 2c). This present study conducted four different
301 experiments to examine the feasibility of using gait disruption patterns to identify safety hazards. They
302 include normal gait (i.e., baseline) without any safety hazard (Experiment 1); normal gait with a slippery
303 surface hazard positioned at 5m from starting point (Experiment 2); normal gait with an obstacle hazard
304 positioned at 5m from the starting point (Experiment 3); and normal gait with an uneven surface hazard
305 positioned at 5m from the starting point (Experiment 4).

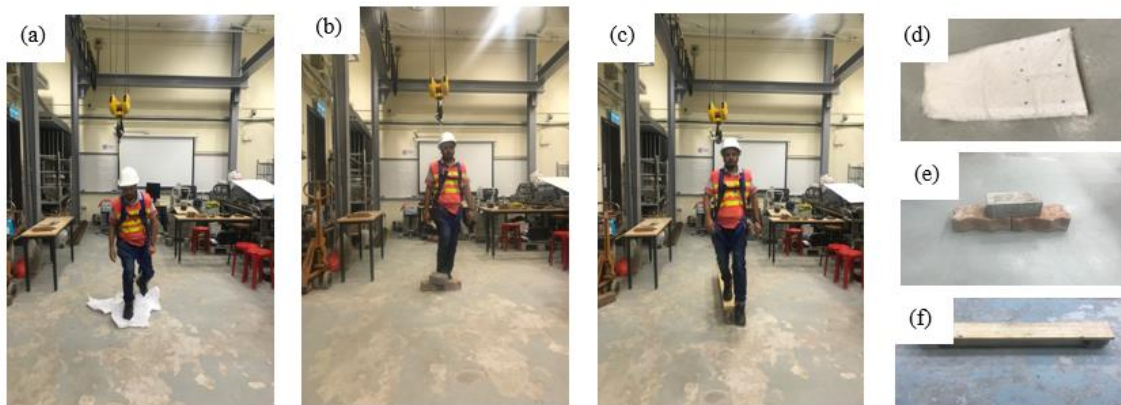
306

307 In all experimental trials, the participants did not have prior knowledge of the location of the safety hazards
308 but were told that there could be an external perturbation during a normal gait. In order for the participant
309 being unable to recognize an unsafe condition and also for them not to avoid a safety hazard on the floor
310 surface, the lights in the laboratory were dimmed and the participants were instructed to look straight ahead
311 during the training session and testing trials. The experimental trials were recorded using a video camcorder,
312 and the video time was synchronized with the timestamps from the wearable insole pressure system. By using
313 the collected video as reference data, the gait cycle under the influence of a safety hazard was manually
314 detected. The sequence of conducting the experimental trials was randomized by means of a random number
315 generator. However, a normal gait was always conducted as a baseline in this study. Each participant
316 performed 10 repetitive randomized trials for each safety hazard (Fig. 1). In order to reduce fatigue, the
317 participants were allowed to rest for 5 minutes between two successive trials (Fig. 1). During the recovery
318 time, the wearable insole pressure sensors were zeroed according to the manufacturer's guidelines.



319

320 **Fig. 1.** A randomized crossover study design in a single testing session.



321

322 **Fig. 2.** Laboratory experiments: (a) slip hazard; (b) trip hazard; (c) unexpected step-down hazard; (d) slippery

323 surface hazard; (e) obstacle hazard; (f) uneven surface hazard.

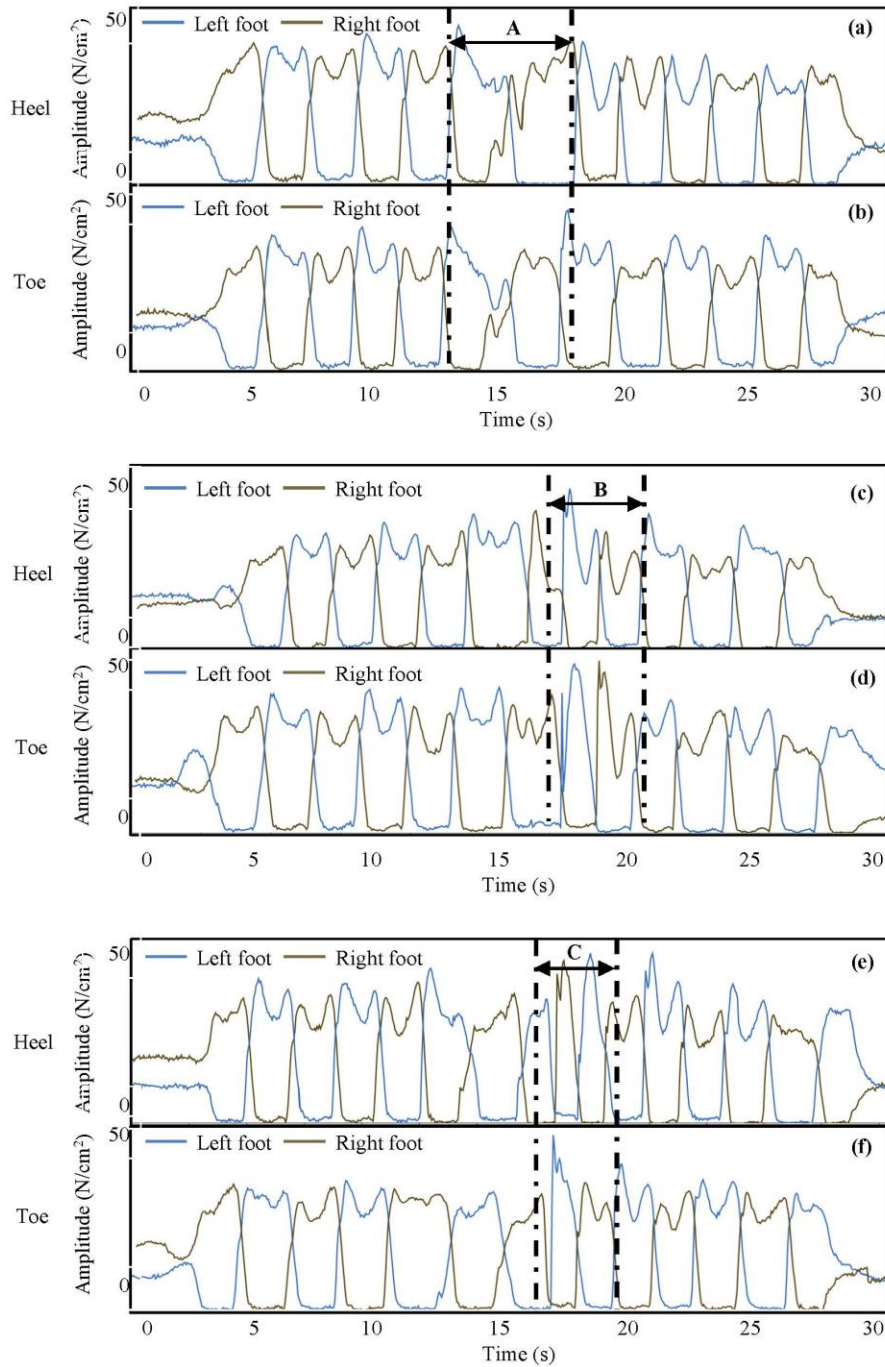
324 *3.4. Data processing and analyses*

325 The raw plantar pressure patterns and GRF data were sampled using a 16-bit analogue to digital converter
326 (ADC) at 50 samples per second for offline analysis. Initially, the raw data was stored in the flash memory
327 of the wearable insoles and they were wirelessly transmitted to a desktop computer (2.80GHz Intel (R) Xeon
328 (R) CPU processor with 4.00GB of RAM). The sampling frequency used in this study was 50Hz (Antwi-
329 Afari et al., 2018e). The experimenter used the live capture data acquisition mode to visually observe the
330 real-time data collection process. In this research, all data processing and analyses were performed using the
331 Statistical Package for the Social Science (SPSS) version 20.0 (IBM, USA). Statistical significance was set
332 at $p < 0.05$.

333
334 In order to compute for gait variability features, gait event detection is the first essential step to detect heel
335 strike and toe-off events during a gait cycle. Heel strike is the moment when the foot makes initial contact
336 with the floor surface after finishing a foot swing during a gait. Toe-off event is the moment when the foot
337 initiates a foot swing during a gait. This study defines a gait cycle as the motion between consecutive heel
338 strikes of the same foot (Hausdorff et al., 1998). In this research, a total of 400 data streams (4 experimental
339 hazard conditions \times 10 repeated trials \times 10 participants) were collected. For each participant, the collected
340 plantar pressure patterns of a single trial during a hazard were used for gait event detection. Consequently,
341 only foot plantar pressure patterns were utilized to identify heel strike and toe-off events in a gait cycle. In
342 order to detect heel strike and toe-off events during a gait cycle, the average pressure was calculated at the
343 heel and toe anatomical foot regions. Based on the four main anatomical foot regions (Choi et al., 2015), the
344 toe region of the foot consists of sensors 14 to 16, whilst the heel region of the foot comprises of sensors 1
345 to 4. Since plantar pressure patterns were collected bilaterally during the experiments, the average pressure
346 sensors from either the left or right foot were both used for detecting gait event. It is worth mentioning that
347 the video time was synchronized with the timestamps of the foot plantar average pressure sensors to aid in
348 detecting gait event.

349
350 Fig. 3 presents the left and right average plantar pressure data at the heel and toe foot regions of a gait cycle
351 in each type of safety hazard. Notably, the heel and toe foot regions were selected because they are the most
352 essential parts of the participants' foot to detect heel strike and toe-off events of a gait cycle so as to compute

353 gait variability parameters. As indicated in Fig. 3, the short-dashed lines represent the defined areas for
354 identifying safety hazards in each hazard condition. Before the participants were being exposed to hazardous
355 conditions, their gait patterns showed continuous and cyclical plantar pressure patterns over time indicating
356 normal gait. During hazard conditions, the participants' gait patterns exhibited exclusive abnormal pressure
357 patterns as denoted as "A", "B" and "C". For example, during a slip hazard, the foot slides forward against
358 the floor, and thus a relatively long pattern of pressure data is found at the heel region as compared to the trip
359 hazard (Fig. 3). During a trip hazard, the participant's foot hits an obstacle to create a very short peak pressure
360 on toe region, and shortly thereafter, higher peak pressure values are found by the other foot which serves to
361 support the body to recover from a trip hazard (Fig. 3). In the unexpected step-down hazard, the length of the
362 participants' gait cycle time decreased as compared to the normal gait (Fig. 3). Based on the analysis of
363 average plantar pressure data, the disruption of participants' gait patterns could enable us to identify safety
364 hazards by quantitatively computing gait variability parameters. In addition, the existence of gait disruption
365 patterns in each foot justifies the need to compute gait variability parameters for each foot during the hazard
366 conditions. By virtue of data preferences, it is evident to mention that foot plantar pressure distribution data
367 collected by wearable insole pressure system can provide a reliable source of data to identify safety hazards
368 in construction. To this end, the current study revealed that the average pressure patterns and duration of the
369 gait cycle of the participants are slightly different in each safety hazard, which may be attributed to the
370 difference in unsafe surface conditions.



371

372 **Fig. 3.** Left and right average pressure amplitude in each hazard condition: (a) Heel pressure during a slip

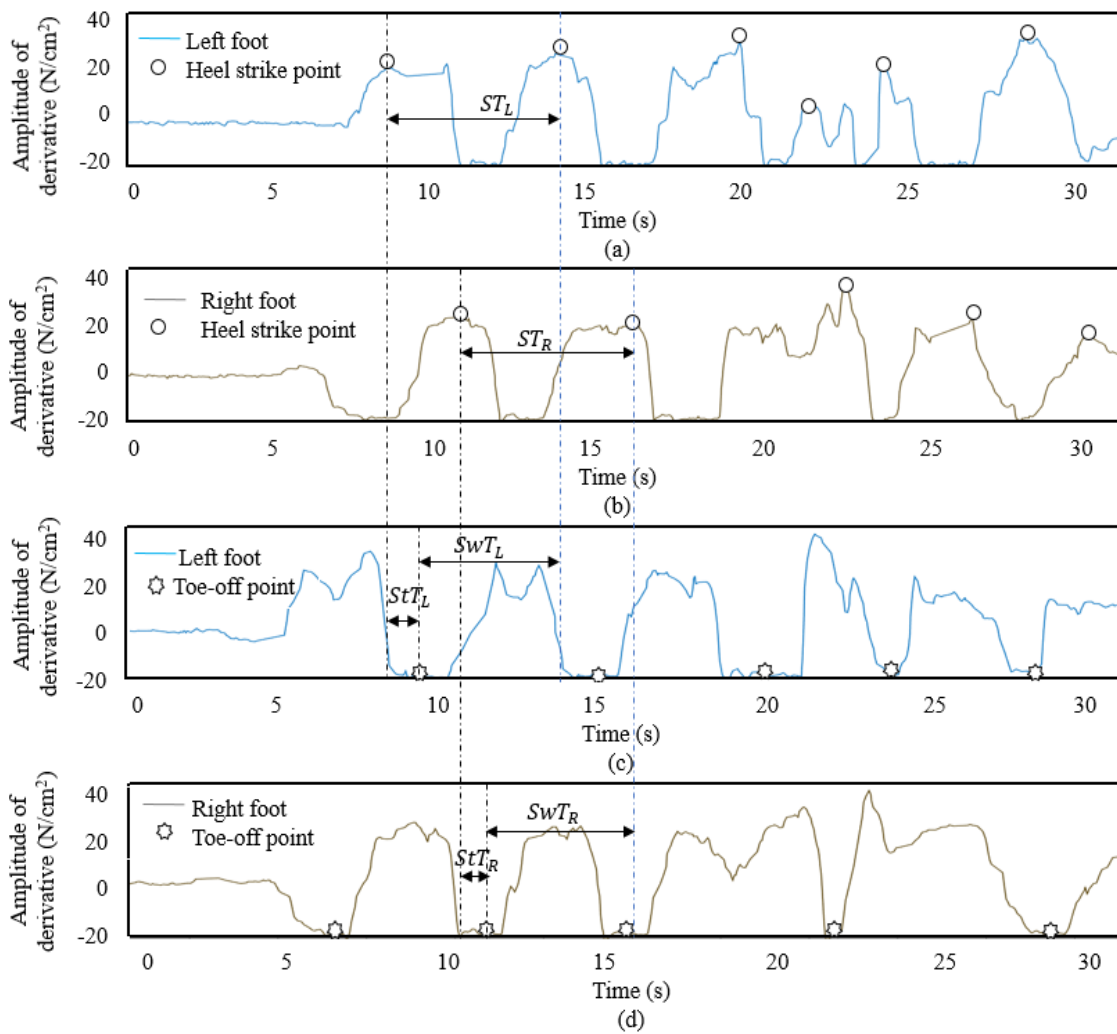
373 hazard; (b) Toe pressure during a slip hazard; (c) Heel pressure during a trip hazard (d) Toe pressure during

374 a trip hazard (e) Heel pressure during an unexpected step-down hazard; and (f) Toe pressure during an

375 unexpected step-down hazard. A = Slippery surface hazard; B = Obstacle hazard; and C = Uneven surface

376 hazard. Dotted lines indicate the defined areas of identifying each hazard condition.

377 Fig. 4 shows the successive derivative of plantar pressure patterns from the heel and toe regions during a slip
 378 hazard. The numeric derivatives of pressure are calculated for the heel strike and toe-off events detection,
 379 which are robust against noisy signals, different offset of the insoles and different weights of participants
 380 (Lin et al., 2016). The authors only presented the successive derivative of plantar pressure patterns during
 381 the slip hazard for simplicity purposes. As shown in Fig. 4, the peak points of the successive derivative
 382 difference of heel plantar pressure patterns from consecutive samples were used to extract heel strike events.
 383 Similarly, the toe-off events were extracted from the trough points of the successive derivative difference of
 384 toe plantar pressure patterns from consecutive samples. Based on heel strike and toe-off events, the present
 385 study computed five gait variability parameters.



386
 387 Fig. 4. The successive derivative of plantar pressure patterns from the heel and toe regions during a slip
 388 hazard: (a) Left foot heel strike; (b) Right foot heel strike; (c) Left foot toe-off; and (d) Right foot toe-off

389 3.4.1. Computation of gait variability parameters

390 This study analyzed five gait variability parameters, namely: stride time, stride length, swing time, stance
391 time, and single support time from the plantar pressure data. As presented in Fig. 4, the stride time (ST) was
392 calculated from the time interval between two successive heel strike events for each of the left and right foot,
393 respectively.

394
$$ST_L = t(LHS_{i+1}) - t(LHS_i) \quad (1)$$

395
$$ST_R = t(RHS_{i+1}) - t(RHS_i) \quad (2)$$

396 Where, ST_L is the stride time of the left foot; ST_R represents the stride time of the right foot; $t(LHS_{i+1})$ and
397 $t(RHS_{i+1})$ represent the time of the $(i + 1)^{th}$ heel strike event for the left foot and right foot, respectively;
398 $t(LHS_i)$ and $t(RHS_i)$ represent the time of the i^{th} heel strike event for the left foot and right foot,
400 respectively.

401

402 The stride length (SL) is the distance covered between two successive heel strike events of the same foot. In
403 order to compute the SL, two basic information such as the ST and the walking speed are needed. To measure
404 a participant's walking speed, this study used the recorded video of the simulated experiments to provide
405 information on the time taken by a participant to complete a single experimental trial. As such, a participant's
406 SL was computed by multiplying the ST and the walking speed (Frenkel-Toledo et al., 2005) for each foot.
407 Consequently, the normalized SL was computed with regards to the participant's height to nullify the effect
408 of inter-subject height differences that can affect one's gait parameters (Elble et al., 1991).

409
$$SL_L = \frac{Walking\ Speed \times ST_L}{Height} \quad (3)$$

410

411
$$SL_R = \frac{Walking\ Speed \times ST_R}{Height} \quad (4)$$

412 Where, SL_L and SL_R are the normalized stride length of the left foot and right foot, respectively.

413

414 Generally, a gait cycle can be divided into two phases, namely; stance and swing phases (O'Sullivan et al.,
415 2019). The stance or swing phases which are associated with a reference foot is either related to the foot
416 being in contact or not in contact with the ground surface, respectively (O'Sullivan et al., 2019). In the present
417 study, stance and swing phases were computed as a percentage of the gait cycle. The measurement of
418 spatiotemporal gait parameters such as percentage of time in swing and stance phases provide important

419 information on the symmetry of a person's gait patterns. Specifically, the period of the stance and swing
 420 phases was used to calculate the percentage of the gait cycle time with reference to each foot. Subsequently,
 421 the swing time was calculated as the time interval between successive toe-off and heel strike events of the
 422 same foot when the foot is not in contact with the ground surface (Fig. 4). Similarly, the stance time was
 423 calculated when the foot is in contact with the ground surface. As shown in Fig. 4, the percentage of the
 424 swing phase (% SwP) and percentage of the stance phase (% StP) were calculated using the swing time (SwT)
 425 and stance time (StT), respectively and quantified as a percentage of the total gait cycle time of the reference
 426 foot (Solanki and Lahiri, 2018).

$$427 \quad \% SwP_L = \frac{t(LHS_{i+1}) - t(LTO_i)}{t(LHS_{i+1}) - t(LHS_i)} \times 100\% \quad (5)$$

$$428 \quad \% SwP_R = \frac{t(RHS_{i+1}) - t(RTO_{i+1})}{t(RHS_{i+1}) - t(RHS_i)} \times 100\% \quad (6)$$

$$430 \quad \% StP_L = \frac{t(LTO_i) - t(LHS_i)}{t(LHS_{i+1}) - t(LHS_i)} \times 100\% \quad (7)$$

$$431 \quad \% StP_R = \frac{t(RTO_{i+1}) - t(RHS_i)}{t(RHS_{i+1}) - t(RHS_i)} \times 100\% \quad (8)$$

432 Where, % SwP_L and % SwP_R represent the percentage of the swing phase of the left foot and right foot;
 433 % StP_L and % StP_R are the percentage of the stance phase of the left foot and right foot; $t(LHS_{i+1})$ and
 434 $t(RHS_{i+1})$ represent the time of the $(i + 1)^{th}$ heel strike event of the left foot and the right foot; $t(LTO_{i+1})$
 435 and $t(RTO_{i+1})$ represent the time of the $(i + 1)^{th}$ toe-off event of the left foot and the right foot; $t(LHS_i)$
 436 and $t(RHS_i)$ are the time of the i^{th} heel strike event of the left foot and the right foot; $t(LTO_i)$ and $t(RTO_i)$
 437 are the time of the i^{th} toe-off event of the left foot and the right foot, respectively.

438
 439
 440
 441 Single support time of a gait cycle is the duration for which only one foot supports the body during a person's
 442 gait (Debi et al., 2011). Alternatively, single support time for a specific foot (i.e., left) can be measured from
 443 the swing time of the other foot (i.e., right) (Bagley et al., 1991). In this study, an alternative approach for
 444 measuring the single support time was adopted. As such, the percentage of single support time (% SST) for
 445 each foot was calculated as a percentage of the total gait cycle time (Solanki and Lahiri, 2018).

446
$$\% SST_L = \frac{t(RHS_{i+1}) - t(RTO_{i+1})}{t(LHS_{i+1}) - t(LHS_i)} \times 100\% \quad (9)$$

447
 448
$$\% SST_R = \frac{t(LHS_{i+1}) - t(LTO_i)}{t(RHS_{i+1}) - t(RHS_i)} \times 100\% \quad (10)$$

449

450 The validity of the computed gait variability parameters was also tested using additional experiments. In
 451 particular, we compared two gait variability parameters such as ST and SL as computed from plantar pressure
 452 patterns with ground truth data that were manually collected using a tape measure and a stopwatch. In this
 453 validating process, a pair of wearable insole pressure sensor was inserted into the participant's safety boots.
 454 The participant conducted a normal gait in a laboratory setting without any safety hazard. The experimenter
 455 collected a total of 50 samples of ST and SL data manually. Then, the ground truth data was compared with
 456 the ST and SL computed from the plantar pressure patterns using root mean square error (RMSE). The
 457 computed ST and SL were within 0.27 s RMSE and 0.07 m RMSE of the ground truth data, respectively,
 458 which equates to less than 7% of the average ST (2.647 s) and SL (1.259 m). In addition, a paired-sample *t*-
 459 test revealed that there was no statistically significant different in normal gait from ground truth data (Mean
 460 = 0.80, SD = 0.13) to ST [Mean = 0.80, SD = 0.13, *t* (49) = 0.868, *p* = 0.390]. The eta squared statistic (0.02)
 461 indicated a moderate effect size (Cohen, 1988). Similarly, a paired-sample *t*-test revealed that there was no
 462 statistically significant different in normal gait from ground truth data (Mean = 1.39, SD = 0.35) to SL [Mean
 463 = 1.38, SD = 0.35, *t* (49) = 1.769, *p* = 0.083]. The eta squared statistic (0.06) indicated a moderate effect size.
 464

465 *3.4.2. Gait abnormality measurement*

466 Several approaches have been studied to measure gait abnormality in clinical and rehabilitation settings.
 467 Examples include but not limited to the Gillette Gait Index (GGI), formerly called the Normalcy Index (Wren
 468 et al., 2007), the Gait Deviation Index (Barton et al., 2015) and Movement Deviation Profile (Barton et al.,
 469 2012). Ultimately, these approaches provide a single score to quantify the disruption of multiple gait features
 470 between healthy participants and patients with disorders such as Parkinson or Cerebral Palsy. Although the
 471 existing approaches achieved accurate results based on joint motions to evaluate gait abnormality, they
 472 require the use of camera-based systems (e.g., 3D cameras, VICON) and reflective markers mounted on
 473 different body parts. As such, they may not be suitable to evaluate gait abnormality of construction workers
 474 on sites. To quantitatively measure a participant's gait abnormality by using GRF data, one of the most widely

475 reported approaches is a force plate (Antwi-Afari et al., 2017a; Antwi-Afari et al., 2017c). However, a force
476 plate requires a well-built walkway and it is usually unmovable. In addition, only one or two steps can be
477 measured during a single trial (Scheepers et al., 2007). To overcome these drawbacks, this study proposes a
478 wearable insole pressure system to capture GRF data as a metric for evaluating participants' gait abnormality
479 when they are exposed to safety hazards in a laboratory setting.

480

481 There are some advantages in using GRF data for evaluating gait abnormality when compared to joint motion
482 data. First, GRF data provides cyclic gait motions in repetitive and unique patterns between the foot and the
483 floor surface, which can serve as a useful indicator for identifying a participant's gait abnormalities. Since
484 the foot is the most distal part of the lower extremity, GRF data patterns contain vital sensor stream
485 information for gait analysis (Bae et al., 2011). In other words, GRF data patterns can easily detect abnormal
486 gait motions during a normal gait. Second, the process of measuring GRF data by using a wearable insole
487 pressure sensor is not only less challenging but also more practical than measuring joint angles from vision-
488 based techniques. This can be explained with regards to privacy issues and data processing. Although
489 previous studies in rehabilitation and clinical settings have utilized GRF data patterns to evaluate gait
490 abnormalities in patients with gait disorders (Scott-Pandorf et al., 2007; Muniz and Nadal, 2009; Bae et al.,
491 2011), no study has attempted to use GRF data to evaluate gait abnormalities when participants are exposed
492 to safety hazards. In this study, gait abnormality based on GRF data is evaluated by how far the gait disruption
493 patterns (i.e., obtained during hazard conditions) is from a normal gait pattern (i.e., no-hazard condition).
494 Since the root-mean-square (RMS) value of the GRF deviation can represent the amount of GRF deviation
495 from the normal gait pattern, gait abnormality is evaluated as the RMS value of GRF deviation normalized
496 by the body weight. Thus, the gait abnormality-based GRF is represented as:

$$497 \quad GA = \frac{1}{BW} \sqrt{\frac{1}{n} \sum_{i=1}^n (GRF_i)^2} \quad (11)$$

498

499 Where GA is the gait abnormality, BW is the participant's body weight, n is the total number of data samples,
500 and GRF_i is the i th GRF deviation.

501

502

503 **4. Results**

504 *4.1. Results of gait variability parameters*

505 This section reports the results of identifying safety hazards based on gait variability parameters. Since our
506 participants were healthy individuals, the results revealed a close agreement of the gait variability parameters
507 between the left foot and right foot. For example, from the first participant, the differences between the left
508 foot and right foot average percentage of swing time during the slip hazard as compared to the normal gait
509 (i.e., no hazard condition) were estimated as -2.2% and -2.3%, respectively. In particular, the non-parametric
510 Wilcoxon Signed-Rank test was conducted to find the statistically significant differences in the average
511 percentage of swing time between the left foot and right foot in each experimental condition. From the first
512 participant, no statistically significant differences in the average percentage of swing time were found
513 between the left foot and right foot during normal gait ($p = 0.279$), slip hazard ($p = 0.126$), trip hazard ($p =$
514 0.192), and unexpected step-down hazard ($p = 0.215$). Since similar results were found in other participants
515 and gait variability parameters, we averaged each gait variability parameter from both feet of each participant
516 to identify the existence of gait disruption in different types of safety hazards.

517

518 Table 2 shows the average gait variability parameters in each hazard condition as compared to normal gait.
519 In each participant, the results revealed that the stride time parameter increases distinctly during all hazard
520 conditions as compared to normal gait. During the slip hazard, most of the participants experienced longer
521 stride times, as such their stride length increased by 1.3% when they encountered a slippery surface hazard
522 (Table 2). The percentage of swing time during the slip hazard conditions decreased by 4.7% as compared to
523 a normal gait (Table 2). In contrast, the percentage of stance time increased by 5.8% during a slip hazard
524 condition when compared to a normal gait (Table 2). Lastly, the single support time increased by 5.1% when
525 participants are exposed to a slip hazard (Table 2).

526

527 With the trip hazard, the participants also had a longer stride time and increased stride length when they
528 encountered the obstacle hazard (Table 2). While the percentage of swing time decreased by 4.4%, the
529 percentage of stance ratio increased by 4.6% when obstacle hazard as compared to a normal gait (Table 2).
530 Lastly, the single support time increased by 4.1% when confronting the obstacle hazard (Table 2).

531 With regards to the [unexpected step-down hazard](#), the participants showed longer stride time and increased
532 stride length similar to both the [slip and trip hazards](#) (Table 2). The percentage of swing time decreased by
533 4.6%, while the percentage of stance time increased by 5.7% when participants were exposed to the uneven
534 surface hazard as compared to a normal gait (Table 2). Lastly, the single support time increased by 4.8%
535 when confronting the uneven surface hazard (Table 2).

Table 2. Average gait variability parameters.

Participant	Stride time (%)				Stride length (%)				Percentage of the swing phase (%)				Percentage of the stance phase (%)				Percentage of the single support time (%)			
	Normal gait	Slip hazard	Trip hazard	Unexpected step-down hazard	Normal gait	Slip hazard	Trip hazard	Unexpected step-down hazard	Normal gait	Slip hazard	Trip hazard	Unexpected step-down hazard	Normal gait	Slip hazard	Trip hazard	Unexpected step-down hazard	Normal gait	Slip hazard	Trip hazard	Unexpected step-down hazard
1	0.92	2.82	2.22	2.62	1.28	2.18	1.68	1.98	2.79	-0.41	-1.51	-5.81	0.22	5.52	2.62	6.72	0.12	2.42	3.62	1.42
2	0.89	3.69	2.49	3.39	1.16	2.46	1.96	1.66	1.98	-0.22	0.08	-2.52	0.31	7.11	8.51	3.91	0.15	6.25	1.95	5.35
3	0.9	4.8	2.4	2.5	1.10	1.80	1.70	1.90	1.47	-4.13	-2.33	-4.93	0.45	6.35	3.25	7.85	0.18	3.48	4.68	2.08
4	0.85	2.35	1.95	2.25	0.98	1.78	1.68	1.48	2.54	-2.56	-2.36	-5.06	0.33	7.03	5.13	4.13	0.21	5.01	1.91	7.51
5	0.87	2.17	2.77	2.67	0.94	2.34	2.54	1.74	2.37	1.17	-1.23	-2.33	0.27	2.77	3.87	7.37	0.17	8.97	4.77	3.67
6	0.93	2.73	3.33	2.53	1.21	2.91	2.01	2.61	1.78	-5.72	-0.52	-1.72	0.42	9.32	5.12	7.32	0.16	5.26	4.46	7.96
7	0.88	3.18	2.48	2.28	1.07	2.67	2.17	2.37	2.23	-1.97	-3.37	0.43	0.35	7.85	2.55	4.65	0.19	6.79	8.09	4.39
8	0.91	2.11	2.71	2.21	0.99	1.79	1.29	1.59	2.49	-3.81	-5.01	-1.61	0.29	3.69	5.89	8.09	0.25	1.55	4.95	2.75
9	0.93	4.03	2.53	2.03	1.07	2.87	1.77	2.27	1.82	-3.88	-2.78	-0.98	0.34	1.54	4.64	7.54	0.16	8.86	1.26	6.06
10	0.78	2.18	2.58	2.08	0.95	2.65	2.15	2.55	2.27	-3.83	-2.83	0.67	0.38	10.08	7.88	2.88	0.24	4.54	7.54	8.34
Average difference \pm SD		2.1 \pm 0.9	1.7 \pm 0.4	1.6 \pm 0.4		1.3 \pm 0.4	0.8 \pm 0.4	0.9 \pm 0.4		-4.7 \pm 2.0	-4.4 \pm 1.6	-4.6 \pm 2.4		5.8 \pm 2.7	4.6 \pm 2.0	5.7 \pm 1.9		5.1 \pm 2.5	4.1 \pm 2.3	4.8 \pm 2.5

Amongst the reported average gait variability parameters for identifying safety hazards as presented in Table 2, the percentage of stance phase showed the greater differences in each hazard condition. This observation may be explained by the fact that the stance phase is considered to be about 60% of a participant's gait cycle for healthy individuals (O'Sullivan et al., 2019). Nevertheless, the overall results confirmed that the existence of gait disruptions measured by gait variability parameters varied either among the participants or between safety hazards. For example, while the [trip hazard](#) found an increased mean difference in stride time as compared to the [unexpected step-down hazard](#), the result found a higher mean difference of stride length, percentage of stance phase, and percentage of single support time in the [unexpected step-down hazard](#) as compared to the [trip hazard](#). On the other hand, the first participant had higher mean stride time in all hazard conditions as compared to the fourth participant. These results indicated that the walking speed and participants' characteristics (e.g., height) have an influence on gait disruption caused by safety hazards. Although the results are promising, the findings are however difficult to determine which gait variability parameter showed a significant difference in identifying safety hazards among construction workers. Overall, the findings of these results revealed the need to measure gait abnormality based on how far the GRF deviations are from the normal gait patterns.

4.2. Gait abnormality measurement based on GRF deviation

By using the GRF data, each participant's gait abnormality was evaluated by comparing the degree of GRF gait disruption in hazard conditions to the GRF patterns during normal gait. Initially, the GRF data samples of the left and right foot were averaged before calculating the gait abnormality of each participant as presented in equation 11. Table 3 shows the average difference in gait abnormality based on GRF deviation in hazard conditions as compared to normal gait. The results of gait abnormality based on GRF deviation found a significant difference ([paired sample \$t\$ -test, \$p < 0.05\$](#)) between hazard conditions and normal gait (Table 3). Generally, it was found that all hazard conditions had higher gait abnormality based on GRF deviation as compared to normal gait. In particular, the obstacle hazard had the highest average difference in gait abnormality (29.05), followed by the uneven surface hazard (22.95) and the slippery surface hazard (17.48), when each hazard condition was compared to normal gait (Table 3). In each participant, there were consistent results of gait abnormality for identifying safety hazards at a specific location (Table 3). While the [trip hazard](#) (i.e., [obstacle hazard](#)) achieved the highest gait disruption from normal gait in each participant, the [slip hazard](#)

obtained the lowest results (Table 3). Taken together, the findings of these results show that the proposed gait abnormality based on GRF deviation is relatively reliable to capture gait disruptions for identifying safety hazards as compared to gait variability parameters computed using plantar pressure patterns.

Table 3. Average difference (standard deviation) in gait abnormality based on ground reaction force (GRF) deviation between each hazard condition (positioned at 5m) and a normal gait.

Participant	Gait abnormality (%)					
	Slippery surface hazard	<i>p</i> -value	Obstacle hazard	<i>p</i> -value	Uneven surface hazard	<i>p</i> -value
1	12.66 (3.17)	0.000	31.79 (5.04)	0.000	24.98 (4.85)	0.000
2	20.78 (13.39)	0.001	42.56 (6.74)	0.000	30.12 (8.40)	0.000
3	13.63 (6.05)	0.000	25.31 (6.22)	0.000	14.91 (5.56)	0.000
4	16.94 (3.88)	0.000	28.69 (5.97)	0.000	19.63 (5.26)	0.000
5	25.58 (5.47)	0.000	40.12 (5.82)	0.000	35.35 (6.78)	0.000
6	10.36 (12.95)	0.032	15.38 (13.36)	0.005	12.65 (14.24)	0.020
7	12.56 (7.89)	0.001	19.47 (7.28)	0.000	15.78 (8.83)	0.000
8	17.89 (3.57)	0.000	27.29 (3.78)	0.000	22.23 (5.76)	0.000
9	13.91 (5.23)	0.000	20.06 (5.21)	0.000	18.19 (5.56)	0.000
10	30.45 (5.16)	0.000	39.87 (7.25)	0.000	35.64 (11.09)	0.000
Mean ± SD	17.48 ± 6.42		29.05 ± 9.47		22.95 ± 8.34	

To verify the performance of safety hazard identification by using the gait abnormality based on GRF deviation, this study conducted the point-biserial correlation analysis between combined gait abnormality based on GRF deviation results of each location and the ground truth on the hazard locations. Table 4 summarizes the point biserial correlation coefficients between the location of a hazard and the average gait abnormality based on GRF deviation. The average gait abnormality based on GRF deviation values showed strong correlations ($r > 0.7$) and significant differences ($p < 0.05$) with obstacle hazard locations, as compared to the uneven surface hazard and slippery surface hazard locations (Table 4). In addition, the correlation coefficient for the obstacle hazard increases faster than the uneven surface and slippery surface hazard locations (Table 4). On the other hand, the composition of the data set also affects the correlation coefficient values. The results showed that the correlation coefficient for the obstacle hazard needed combined data set from 4 participants (40 trials) to obtain a strong correlation ($r > 0.7$) with average gait abnormality based on GRF deviation, whereas the uneven surface hazards and slippery surface hazards required combined data set from 5 participants (50 trials) and 6 participants (60 trials), respectively. Ultimately, the strong correlation coefficients in the hazard conditions indicate that participants' gait disruptions are abnormal and strongly

dispersed when exposed to a safety hazard. These findings indicated that with a sufficient number of data samples, the proposed gait abnormality based on GRF deviation could be feasible to identify safety hazards in construction.

Table 4. Point biserial correlation coefficient between average gait abnormality based on GRF deviation and hazard location (positioned at 5m from starting point).

Participants	Point biserial correlation coefficient		
	Slippery surface hazard	Obstacle hazard	Uneven surface hazard
1	0.712*	0.945*	0.822*
2	0.789*	0.936*	0.863*
3	0.745*	0.978*	0.886*
4	0.763*	0.914*	0.812*
5	0.614	0.956*	0.638
6	0.765*	0.941*	0.835*
7	0.793*	0.922*	0.864*
8	0.771*	0.973*	0.896*
9	0.743*	0.965*	0.864*
10	0.629	0.919*	0.844*

*Indicates a strong correlation

The present study also examined the size of the data set and the diversity of data sources by using gait abnormality based GRF deviation results for identifying safety hazards. In order to conduct this analysis, the number of experimental trials for each participant was fixed at ten, and the number of participants increased from 1 to 10. Fig. 5 (a) to (d) illustrate the box plots of average gait abnormality based GRF deviation values from all possible combinations by increasing the number of participants during normal gait (i.e., no hazard condition) (Fig. 5a), slippery surface hazard (Fig. 5b), obstacle hazard (Fig. 5c), and uneven surface hazard (Fig. 5d) conditions. To prevent sample bias in each experimental condition, the average of the possible sample selection was evaluated in the present study. As shown in Fig. 5, the vertical axis represents the average of aggregated gait abnormality based GRF deviation values whilst the horizontal axis indicates the number of participants. For instance, “P1” in Fig. 5 shows the distribution of aggregation gait abnormality based GRF deviation mean values from one participant out of all the ten participants. Similarly, “P2” and “P3” in Fig. 5 represents the average distribution of aggregation gait abnormality based GRF deviation values from all the possible selections of two participants (e.g., participant 1 and 2; participant 2 and 3) and three participants (e.g., participant 1, 2, and 3; participant 2, 3, and 4), respectively. Any overlaps of the boxplots between a normal gait condition and each hazard condition indicate a possible false detection in identifying

hazards by using gait abnormality based GRF deviation values. Although the results showed false detection by comparison (i.e., normal gait vs slippery surface hazard, normal gait vs obstacle hazard, and normal gait vs uneven surface hazard), it was found that increasing the number of participants is highly effective in reducing false detection and that the slippery surface and the uneven surface hazards require more gait abnormality based GRF deviation values aggregation compared to the obstacle hazard. In addition, the average distribution of aggregated gait abnormality based GRF deviation values increased gradually as more participants were added. It was revealed that the obstacle hazard had the highest average aggregation of gait abnormality based GRF deviation values as compared to the uneven surface hazard and the slippery surface hazard (i.e., the lowest).

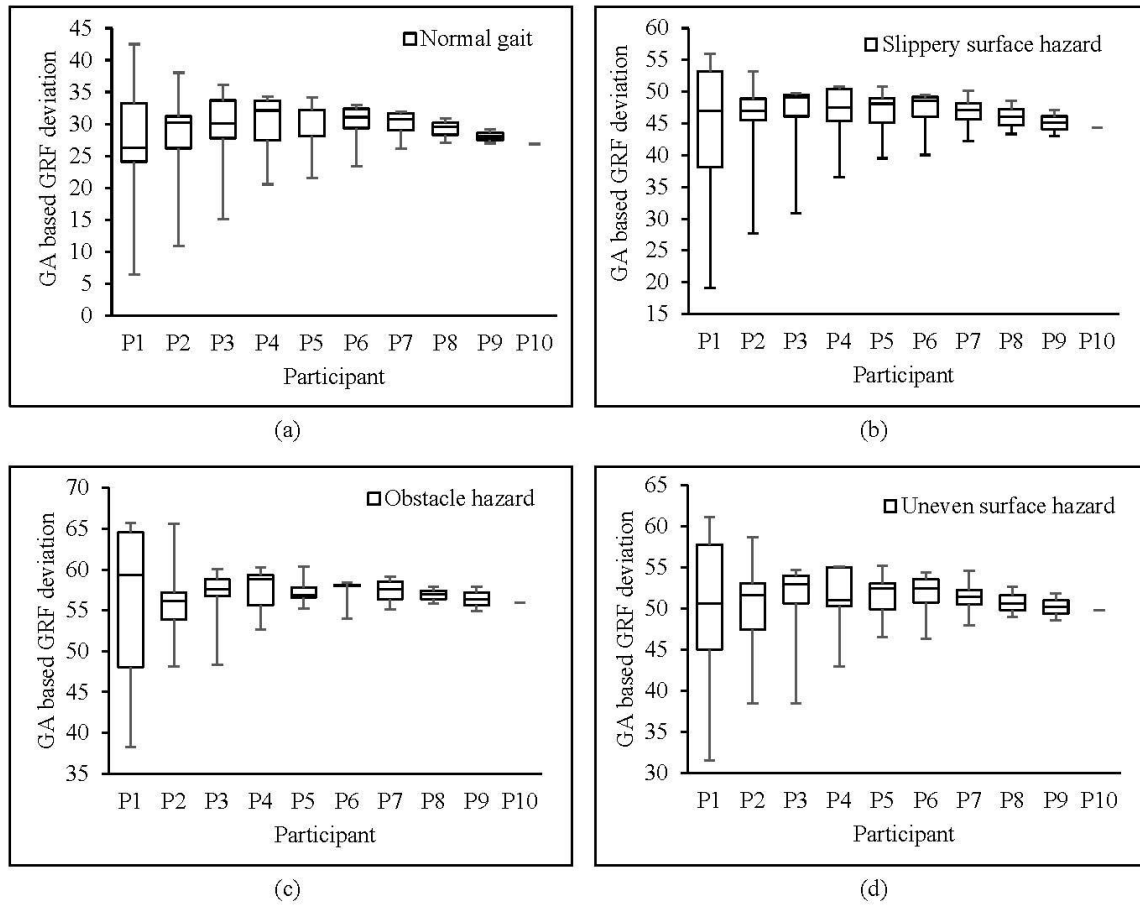


Fig. 5. Box plots of average gait abnormality based GRF deviation values from all possible combinations by increasing the number of participants: (a) normal gait (no hazard condition), (b) slippery surface hazard, (c) obstacle hazard, and (d) uneven surface hazard.

5. Discussion

Amongst the various causes of occupational injuries, [slips, trips, and unexpected step-down hazards](#) have been recognized as a major cause of non-fatal fall injuries in construction. To mitigate these accidents in construction, safety hazard identification is an essential step to recognize hazards and implement proactive fall-preventive interventions. Therefore, the present study proposes a novel and non-intrusive approach—such a wearable insole pressure system—to examine the changes in workers’ gait disruption patterns to identify safety hazards [among construction workers](#). A simulated laboratory study was conducted to test the feasibility of using participants’ gait abnormalities to identify safety hazards. The results found gait variability parameters [could serve as useful](#) gait metrics for identifying workers’ gait [disruption patterns](#) caused by safety hazards. In addition, the gait abnormality based on GRF deviation values provided a significant difference in identifying safety hazards as compared to [normal gait \(i.e., no hazard condition\)](#). [In addition](#), the point biserial correlation coefficients between the presence of a hazard and the average gait abnormality based on GRF deviation showed a strong correlation with obstacle hazard, as compared to correlations with the hazard locations of [uneven surface hazard and slippery surface hazard](#). [Lastly, the obstacle hazard had the highest average aggregation of gait abnormality based GRF deviation values as compared to the uneven surface hazard and the slippery surface hazard](#). Overall, the implications of the current study could greatly enhance existing approaches of safety hazard identification and may also be useful to safety managers to implement proactive fall-prevention strategies.

This study computed five gait variability parameters to evaluate the disruption of a participant’s gait pattern in order to identify safety hazards. Although gait variability parameters were showed as useful gait metric between the existence of a gait disruption caused by a hazard and a normal gait, the percentage of stance phase achieved the greatest difference in gait disruption mainly between an obstacle hazard and a normal gait. Despite the importance of these findings, gait variability parameters could not provide enough sensitive to identify safety hazards. To address the aforementioned drawback, the current study proposed the gait abnormality based on GRF deviation for evaluating the disruption of a participant’s gait patterns to identify safety hazards. Our results showed that the disruptions caused by obstacle hazard achieved the highest gait abnormality based on GRF deviation values, followed by [uneven surface hazard and slippery surface hazard](#) [when each hazard condition was compared to a normal gait](#). Furthermore, the average gait abnormality based

on GRF deviation values showed strong correlations ($r > 0.7$) with obstacle hazard locations, as compared to correlations with the hazard locations of the [uneven surface hazard and slippery surface hazard](#). Moreover, [the diversity of data source and size of data set indicated that the obstacle hazard had the highest average aggregation of gait abnormality based GRF deviation values as compared to the uneven surface hazard and the slippery surface hazard](#). These results confirmed the hypothesis that gait abnormality based on GRF deviation in a specific location has a strong relationship with the presence of a hazard in that location. Taken together, the proposed gait abnormality based on GRF deviation is more sensitive than the computed gait variability parameters for identifying the presence of hazards.

It may be difficult to compare our novel approach for identifying hazards with the findings from previous studies. Notably, this research computed five gait variability parameters, namely stride time, stride length, swing time, stance time, and single support time to identify hazards. In addition, the present study proposed gait abnormality based on GRF deviation for measuring the disruption of a participant's gait patterns to identify safety hazards. Moreover, three types of hazards were tested and compared to a normal gait to identify safety hazards in a simulated laboratory setting. It is very obvious that our experimental design has several methodological differences from previous studies with regards to the differences in the experimental protocol, participants' physiological characteristics, data collection procedure, type of wearable sensing systems and the nature of safety hazards. For example, in the construction realm, Kim et al. (2016) and Yang et al. (2017) had examined the feasibility of analyzing collective patterns of workers' bodily responses to identify safety hazards on a job site. These authors conducted laboratory experiments simulating an ironworker's working environment to collect kinematic gait data by using WIMU-based systems. Their findings highlight the opportunity for using workers' abnormal gait responses to identify safety hazards in diverse construction environments. In a clinical setting, Li et al. (2018) investigated the feasibility and comparison of gait parameters such as normalized foot peak pressure, stance ratio, walking velocity, step-time variability using wearable shoes fused with range sensor arrays and other methods. Their results show a significantly less stride length and walking velocity, higher stance ratio and step-time variability in the abnormal gait as compared to normal gait. In rehabilitation, Bae et al. (2011) proposed a mobile gait monitoring system to monitor Parkinson disease patients' gait by observing the GRF and analyzing their gait

abnormality. Their proposed system could help patients to correct their gait by providing them with feedback information. Despite these differences, the findings from the current study show similar results with previous studies (Bae et al., 2011; Kim et al., 2016; Yang et al., 2017; Li et al., 2018; Solanki and Lahiri, 2018). Taken together, the findings have demonstrated the importance of analyzing participants' gait disruption for identifying safety hazards in construction and improving patients suffering from gait disorders.

6. Implications and potential applications

The current study presents the first effort to propose a non-invasive approach to examine the changes in workers' gait abnormalities to identify safety hazards. The findings have theoretical and practical implications for construction safety. First, the results provide novel evidence suggesting that gait disruptions caused by safety hazards could be identified using a wearable insole pressure system. More specifically, the proposed gait abnormality based on GRF deviation found significant evidence suggesting that the presence of a hazard has a strong relationship with a participant's gait response. Consequently, the results of this study would enhance safety managers' hazard identification capabilities to implement proactive fall-prevention interventions in order to mitigate latent hazards on site. Second, this current research proposes a novel approach of using a wearable insole pressure system for analyzing workers' gait abnormalities to identify hazards. Previous safety hazard identification methods (e.g., job-hazard analyses, safety checklists, safety training) are limited because they are unable to continuously identify hazards due to different levels of experts' knowledge, experience and dynamic construction environment. Thanks to the proposed approach which is feasible to address the given limitations. Eventually, it could extend the existing methods of safety hazard identifications for preventing non-fatal fall injuries among construction workers. In summary, the proposed approach can serve as a great potential for developing a continuous and an automated hazard identification system that uses workers' gait response as an informative source of data for recognizing hazard on construction sites. Third, our approach has some practical and economic benefits as compared to current safety hazard identification methods such as the use of WIMU-based systems. It is light-weight, cost-effective and convenient to use since it can be easily inserted or detached to a worker's safety boots. Also, it can be wirelessly connected to computers, smartphones, or other location-tracking systems for its applications in both indoor and outdoor environments. Moreover, it causes less constraint in body movement and minimizes discomfort. Collectively, it is non-intrusive and can allow safety managers to deeply

understand the dynamics of foot mechanisms caused by hazards on construction sites in order to implement proactive fall-prevention interventions.

7. Limitations and future directions

Despite the study contributions, there are some limitations that need to be addressed in future research. First, this study was conducted in a laboratory setting with a small sample of student participants. Future research is warranted to compare the findings of this study with a large sample of experienced construction workers from different construction trades. Moreover, future research should evaluate the reliability of the proposed approach in real-world settings. Second, our experiment was conducted to only include three types of hazards on construction sites. Other types of hazards or fall risk factors should be examined in the future. For example, future works should examine the effect of individual factors (e.g., work experience, age, gender) and other intrinsic risk factors (e.g., fatigue) on workers' gait responses using the proposed approach. In addition, the conducted experiment excluded workers' activities such as lifting, carrying, pulling, pushing. Future research is needed to investigate the changes in workers' gait disruption caused by other types of hazards and activities using the proposed approach. Moreover, different types of gait variability parameters such as average velocity, maximum foot clearance, cadence need to be computed to provide more robust information for identifying hazards. Third, despite its great potential as a tool for automated safety hazard identification, future studies will need to validate the proposed approach before being ready for use in practical applications. Furthermore, it would be beneficial to integrate other sensing and localization technologies such as light sensors, ultra-wideband and cameras with the proposed approach in order to provide more robust application solutions for construction workers' safety. For example, workers' gait responses based on the proposed methodology could be integrated with two-dimensional spatial information captured from the ultra-wideband location technique to provide the location of safety hazards on construction sites. [Lastly, the effects of extrinsic risk factors such as environmental weather conditions, types of footwear, rainwater, lighting, and sweat on changes in foot plantar pressure patterns captured by a wearable insole pressure system during construction workers' activities had not been explored. Taken together, future research studies are warranted to explore the aforementioned extrinsic risk factors to gain a deeper understanding of the changes in gait patterns to extend the practical applications of the proposed approach.](#)

8. Conclusions

The current study proposed a non-invasive approach to examine the feasibility of using workers' gait disruption patterns to identify safety hazards among construction workers. It was hypothesized that workers' gait disruption in a specific location has a strong relationship with the presence of a hazard in that location. To test the hypothesis, ten healthy participants were recruited to perform simulated experiments in a laboratory setting by installing three types of hazards which are common in a construction job site. Consequently, the participants' gait patterns were measured using a wearable insole pressure system to compute five gait variability parameters and a gait abnormality based on GRF deviation to identify the existence of a safety hazard. The results found that gait variability parameters could serve as useful gait metrics for identifying workers' gait disruptions caused by a safety hazard. Alternatively, the gait abnormality based on GRF deviation values provided significant differences in identifying safety hazards in each hazard condition as compared to a normal gait condition. Moreover, the results indicated that participants' gait disruptions measured by the average gait abnormality based on GRF deviation values are highly correlated with the location of a hazard. Lastly, the diversity of data source and size of data set indicated that the obstacle hazard had the highest average aggregation of gait abnormality based GRF deviation values as compared to the uneven surface hazard and the slippery surface hazard.

The findings of this study highlight the feasibility of identifying safety hazards based on workers' gait disruption patterns and potential applications of using a wearable insole pressure system to continuously monitor hazards without interfering with construction workers activities. Moreover, the findings can enhance safety managers' hazard identification capabilities for detecting safety hazards and could help them to implement proactive fall-prevention interventions to eliminate hazards on the job site. Furthermore, these findings provide the basis for developing a non-intrusive and automated wearable insole pressure system that uses workers' gait disruption patterns as a useful data source for safety hazard identification in construction. Lastly, this study extends the use of wearable sensing technologies for mitigating non-fatal fall injuries and improve workers' safety research in construction. Overall, the key contribution of this paper relies on the use of a non-invasive wearable insole pressure system as a real-time monitoring approach to analysis participants' gait disruption patterns for construction safety hazard identification.

Data Availability Statement

All data generated or analyzed that support the findings of this study are available from the corresponding author upon request.

Acknowledgements

The authors acknowledged the support from the Department of Building and Real Estate of The Hong Kong Polytechnic University, the General Research Fund (GRF) Grant (BRE/PolyU 152047/19E) entitled “In Search of a Suitable Tool for Proactive Physical Fatigue Assessment: An Invasive to Non-invasive Approach”. Special thanks are given to Mr Wong Chun Fai for assisting with the experiments and all our participants involved in this study.

Declarations of interest

None

References

- Akhavian, R., and Behzadan, A. H. (2016) Smartphone-Based Construction Workers' Activity Recognition and Classification, *Automation in Construction*, Vol. 71, No. 2, pp. 198-209. DOI: <https://doi.org/10.1016/j.autcon.2016.08.015>.
- Albert, A., Hallowell, M. R., and Kleiner, B. M. (2014b) Experimental Field Testing of a Real-Time Construction Hazard Identification and Transmission Technique, *Construction Management and Economics*, Vol. 32, No. 10, pp. 1000–1016. DOI: <https://doi.org/10.1080/01446193.2014.929721>.
- Albert, A., Hallowell, M. R., Kleiner, B., Chen, A., and Golparvar-Fard, M. (2014a) Enhancing Construction Hazard Recognition with High-Fidelity Augmented Virtuality, *Journal of Construction Engineering Management*, Vol. 140, No. 7, pp. 4014024. DOI: [https://doi.org/10.1061/\(ASCE\)CO.1943-7862.0000860](https://doi.org/10.1061/(ASCE)CO.1943-7862.0000860).
- Antwi-Afari, M. F. (2019) Evaluation of Biomechanical Risk Factors for Work-Related Musculoskeletal Disorders and Fall Injuries among Construction Workers, PhD Thesis, Department of Building and Real Estate, The Hong Kong Polytechnic University.
- Antwi-Afari, M. F., and Li, H. (2018g) Fall Risk Assessment of Construction Workers Based on Biomechanical Gait Stability Parameters Using Wearable Insole Pressure System, *Advanced Engineering Informatics*, Vol. 38, pp. 683-694. DOI: <https://doi.org/10.1016/j.aei.2018.10.002>.
- Antwi-Afari, M. F., Li, H., Edwards, D. J., Pärn, E. A., Owusu-Manu, D., Seo, J., and Wong, A. Y. L. (2018a) Identification of Potential Biomechanical Risk Factors for Low Back Disorders During Repetitive Rebar Lifting, *Construction Innovation: Information, Process, Management*, Vol. 18, No. 2. DOI: <https://doi.org/10.1108/CI-05-2017-0048>.
- Antwi-Afari, M. F., Li, H., Edwards, D. J., Pärn, E. A., Seo, J., and Wong, A. Y. L. (2017b) Biomechanical Analysis of Risk Factors for Work-Related Musculoskeletal Disorders During Repetitive Lifting Task in Construction Workers, *Automation in Construction*, Vol. 83, pp. 41-47. DOI: <https://doi.org/10.1016/j.autcon.2017.07.007>.
- Antwi-Afari, M. F., Li, H., Edwards, D. J., Pärn, E. A., Seo, J., and Wong, A. Y. L. (2017a). Effects of Different Weight and Lifting Postures on Postural Control During Repetitive Lifting Tasks, *International Journal of Building Pathology and Adaptation*, Vol. 35, No. 3, pp. 247-263. DOI: <https://doi.org/10.1108/IJBPA-05-2017-0025>.
- Antwi-Afari, M. F., Li, H., Luo, X. E., Edwards, D. J., Owusu-Manu, D., and Darko, A. (2019c) Overexertion-Related Construction Workers' Activity Recognition and Ergonomic Risk Assessment Based on Wearable Insole Pressure System. Proceeding of 8th West Africa Built Environment Research (WABER) Conference, Accra, Ghana, August 5-7, 2019. Available via: <https://www.researchgate.net/publication/335570297>(Accessed: March 2020).
- Antwi-Afari, M. F., Li, H., Seo, J., and Wong, A. Y. L. (2017c). Effects of Quadriceps Muscle Fatigue on Balance Control and Fall Injuries Following Repetitive Squat Lifting Task in Construction Workers. Proceedings of 7th West Africa Built Environment Research (WABER) Conference, Accra, Ghana, August 16-18, 2017. Available via: <https://www.researchgate.net/publication/319939268>(Accessed: March 2020).

- Antwi-Afari, M. F., Li, H., Seo, J., and Wong, A. Y. L. (2018e) Automated Detection and Classification of Construction Workers' Loss of Balance Events Using Wearable Insole Pressure Sensors, *Automation in Construction*, Vol. 96, pp. 189-199. DOI: <https://doi.org/10.1016/j.autcon.2018.09.010>.
- Antwi-Afari, M. F., Li, H., Seo, J., Lee, S., Edwards, D. J., and Wong, A. Y. L. (2018c) Wearable Insole Pressure Sensors for Automated Detection and Classification of Slip-Trip-Loss-Of-Balance Events in Construction Workers. *Construction Research Congress*, New Orleans, Louisiana, USA, April 2-5, 2018. DOI: <https://doi.org/10.1061/9780784481288.008>.
- Antwi-Afari, M. F., Li, H., Wong, J. K. W., Oladinrin, O. T., Ge, J. X., Seo, J., and Wong, A. Y. L. (2019a) Sensing and Warning-Based Technology Applications to Improve Occupational Health and Safety in the Construction Industry: A Literature Review, *Engineering, Construction and Architectural Management*. DOI: <https://doi.org/10.1108/ECAM-05-2018-0188>.
- Antwi-Afari, M. F., Li, H., Yu, Y., and Kong, L. (2018f) Wearable Insole Pressure System for Automated Detection and Classification of Awkward Working Postures in Construction Workers, *Automation in Construction*, Vol. 96, pp. 433-441. DOI: <https://doi.org/10.1016/j.autcon.2018.10.004>.
- Bae, J., Kong, K., Byl, N., and Tomizuka, M. (2011) A Mobile Gait Monitoring System for Abnormal Gait Diagnosis and Rehabilitation: A Pilot Study for Parkinson Disease Patients, *Journal of Biomechanical Engineering*, Vol. 133, No. 4, pp. 041005. DOI: <https://doi.org/10.1115/1.4003525>.
- Bagley, S., Kelly, B., Tunncliffe, N., Turnbull, G. I., and Walker, J. M. (1991) The Effect of Visual Cues on the Gait of Independently Mobile Parkinson's Disease Patients, *Physiotherapy*, Vol. 77, No. 6, pp. 415-420. DOI: [https://doi.org/10.1016/S0031-9406\(10\)62035-4](https://doi.org/10.1016/S0031-9406(10)62035-4).
- Barton, G. J., Hawken, M. B., Holmes, G., and Schwartz, M. H. (2015) A Gait Index May Underestimate Changes of Gait: A Comparison of the Movement Deviation Profile and the Gait Deviation Index, *Computer Methods in Biomechanics and Biomedical Engineering*, Vol. 18, No. 1, pp. 57-63. DOI: <https://doi.org/10.1080/10255842.2013.776549>.
- Barton, G. J., Hawken, M. B., Scott, M. A., and Schwartz, M. H. (2012) Movement Deviation Profile: A Measure of Distance from Normality Using a Self-Organizing Neural Network, *Human Movement Science*, Vol. 31, No. 2, pp. 284-294. DOI: <https://doi.org/10.1016/j.humov.2010.06.003>.
- Boyle, J., Karunanithi, T., Wark, T., Chan, W., and Colavitti, C. (2006) Quantifying Functional Mobility Progress for Chronic Disease Management, 2006 International Conference of the IEEE Engineering in Medicine and Biology Society, New York, USA, 30 August to 3 September 2006, pp. 5916-5919. DOI: <https://doi.org/10.1109/IEMBS.2006.260426>.
- Bureau of Labor Statistics (BLS) (2015) *Census of Fatal Occupational Injuries - Current and Revised Data*. Available at: <http://www.bls.gov/iif/oshcfoi1.htm> (Accessed in October 2019).
- Bureau of Labor Statistics (BLS) (2017) *Injuries, Illnesses, and Fatalities*. Available at: <https://www.bls.gov/iif/> (Accessed: October 2019).
- Carter, G., and Smith, S. D. (2006) Safety Hazard Identification on Construction Projects, *Journal of Construction Engineering and Management*, Vol. 132, No. 2, pp. 197-205. DOI: [https://doi.org/10.1061/\(ASCE\)0733-9364\(2006\)132:2\(197\)](https://doi.org/10.1061/(ASCE)0733-9364(2006)132:2(197)).
- Center for Construction Research and Training (CPWR) (2013) *The Construction Chart Book: The United States Construction Industry and Its Workers*, 5th Ed., Silver Spring, MD. Available at: https://www.cpwr.com/sites/default/files/research/CB4_Final%20for%20web.pdf (Accessed: October 2019).
- Chi, C. F., Chang, T. C., and Ting, H. I. (2005) Accident Patterns and Prevention Measures for Fatal Occupational Falls in the Construction Industry, *Applied Ergonomics*, Vol. 36, No. 4, pp. 391-400. DOI: <https://doi.org/10.1016/j.apergo.2004.09.011>.
- Choi, S., Cho, H., Kang, B., Lee, D. H., Kim, M. J., and Jang, S. H. (2015) Slip-Related Changes in Plantar Pressure Distribution, and Parameters for Early Detection of Slip Events, *Annals of Rehabilitation Medicine*, Vol. 39, No. 6, pp. 897-904. DOI: <https://doi.org/10.5535/arm.2015.39.6.897>.
- Cohen, J. (1988) *Statistical Power Analysis for The Behavioral Sciences*. 2nd Edition, Hillsdale, NJ: Erlbaum. ISBN 0-8058-0283-5.
- Culhane, K. M., O'connor, M., Lyons, D., and Lyons, G. M. (2005) Accelerometers in Rehabilitation Medicine for Older Adults, Age and Ageing, Vol. 34, No. 6, pp. 556-560. DOI: <https://doi.org/10.1093/ageing/afi192>.
- David, V., Forjan, M., Martinek, J., Kotzian, S., Jagos, H., and Rafolt, D. (2017) Evaluating Wearable Multimodal Sensor Insoles for Motion-Pattern Measurements in Stroke Rehabilitation—A Pilot

- Study, In 2017 International Conference on Rehabilitation Robotics (ICORR), London, UK, July 17-20, 2017. pp. 1543-1548. DOI: <https://doi.org/10.1109/ICORR.2017.8009467>.
- Debi, R., Mor, A., Segal, G., Segal, O., Agar, G., Debbi, E., Halperin, N., Haim, A., and Elbaz, A. (2011) Correlation Between Single Limb Support Phase and Self-Evaluation Questionnaires in Knee Osteoarthritis Populations, *Disability and Rehabilitation*, Vol. 33, No. 13-14, pp. 1103-1109. DOI: <https://doi.org/10.3109/09638288.2010.520805>.
- Decker, L., Houser, J. J., Noble, J. M., Karst, G. M., and Stergiou, N. (2009) The Effects of Shoe Traction and Obstacle Height on Lower Extremity Coordination Dynamics During Walking, *Applied Ergonomics*, Vol. 40, No. 5, pp. 895–903. DOI: <http://dx.doi.org/10.1016/j.apergo.2008.12.005>.
- Development Bureau, The Government of the Hong Kong SAR (2017) Accident Statistics and Analyses for Public Works Contracts 2016. Available via: https://www.devb.gov.hk/filemanager/en/content_32/2016_Annual_Report.pdf (Accessed in October 2019).
- Dong, X. S., Fujimoto, A., Ringen, K., and Men, Y. (2009). Fatal Falls Among Hispanic Construction Workers, *Accident Analysis & Prevention*, Vol. 41, No. 5, pp. 1047-1052. DOI: <https://doi.org/10.1016/j.aap.2009.06.012>.
- Dzeng, R. J., Fang, Y. C., and Chen, I. C. (2014) A Feasibility Study of Using Smartphone Built-In Accelerometers to Detect Fall Portents, *Automation in Construction*, Vol. 38, pp. 74–86. DOI: <https://doi.org/10.1016/j.autcon.2013.11.004>.
- Elble, R. J., Thomas, S. S., Higgins, C., and Colliver, J. (1991) Stride-Dependent Changes in Gait of Older People, *Journal of Neurology*, Vol. 238, No. 1, pp. 1-5. DOI: <https://doi.org/10.1007/BF00319700>.
- Frenkel-Toledo, S., Giladi, N., Peretz, C., Herman, T., Gruendlinger, L., and Hausdorff, J. M. (2005) Effect of Gait Speed on Gait Rhythmicity in Parkinson's Disease: Variability of Stride Time and Swing Time Respond Differently, *Journal of NeuroEngineering and Rehabilitation*, Vol. 2, No. 1, pp. 23. DOI: <https://doi.org/10.1186/1743-0003-2-23>.
- Goh, Y., and Chua, D. (2009) Case-Based Reasoning for Construction Hazard Identification: Case Representation and Retrieval, *Journal of Construction Engineering and Management*, Vol. 135, No. 11, pp. 1181-1189. DOI: [https://doi.org/10.1061/\(ASCE\)CO.1943-7862.0000093](https://doi.org/10.1061/(ASCE)CO.1943-7862.0000093).
- Han, S., and Lee, S. (2013) A Vision-Based Motion Capture and Recognition Framework for Behavior-Based Safety Management, *Automation in Construction*, Vol. 35, pp. 131–141. DOI: <http://dx.doi.org/10.1016/j.autcon.2013.05.001>.
- Han, S., Lee, S., and Peña-Mora, F. (2012) Vision-Based Detection of Unsafe Actions of a Construction Worker: A Case Study of Ladder Climbing, *Journal of Computing in Civil Engineering*, Vol. 27, No. 6, pp. 635-644. DOI: [https://doi.org/10.1061/\(ASCE\)CP.1943-5487.0000279](https://doi.org/10.1061/(ASCE)CP.1943-5487.0000279).
- Harle, R., Taherian, S., Pias, M., Coulouris, G., Hopper, A., Cameron, J., Lasenby, J., Kuntze, G., Bezodis, I., Irwin, G., and Kerwin, D. G. (2012) Towards Real-Time Profiling of Sprints Using Wearable Pressure Sensors, *Computer Communications*, Vol. 35, No. 6, pp. 650-660. DOI: <https://doi.org/10.1016/j.comcom.2011.03.019>.
- Hausdorff, J. M., Cudkowicz, M. E., Firtion, R., Wei, J. Y., and Goldberger, A. L. (1998) Gait Variability and Basal Ganglia Disorders: Stride-To-Stride Variations of Gait Cycle Timing in Parkinson's Disease and Huntington's Disease, *Movement Disorders*, Vol. 13, No. 3, pp. 428-437. DOI: <https://doi.org/10.1002/mds.870130310>.
- Howcroft, J., Kofman, J., and Lemaire, E. D. (2013) Review of Fall Risk Assessment in Geriatric Populations Using Inertial Sensors, *Journal of NeuroEngineering and Rehabilitation*, Vol. 10, No. 1, pp. 91. DOI: <https://doi.org/10.1186/1743-0003-10-91>.
- Howcroft, J., Kofman, J., Lemaire, E. D., and McIlroy, W. E. (2016) Analysis of Dual-Task Elderly Gait in Fallers and Non-Fallers Using Wearable Sensors, *Journal of Biomechanics*, Vol. 49, No. 7, pp. 992-1001. DOI: <https://doi.org/10.1016/j.jbiomech.2016.01.015>.
- International Labor Organization (ILO) (2016) Safety and Health at Work. Available at: <https://www.ilo.org/global/topics/safety-and-health-at-work/lang--en/index.htm> (Accessed: October 2019).
- Jebelli, H., Ahn, C. R., and Stentz, T. L. (2016a) Comprehensive Fall-Risk Assessment of Construction Workers Using Inertial Measurement Units: Validation of the Gait-Stability Metric to Assess the Fall Risk of Iron Workers, *Journal of Computing in Civil Engineering*, Vol. 30, No. 3, pp. 04015034. DOI: [http://doi.org/10.1061/\(ASCE\)CP.1943-5487.0000511](http://doi.org/10.1061/(ASCE)CP.1943-5487.0000511).

- Kaskutas, V., Dale, A. M., Lipscomb, H., and Evanoff, B. (2013) Fall Prevention and Safety Communication Training for Foremen: Report of A Pilot Project Designed to Improve Residential Construction Safety, *Journal of Safety Research*, Vol. 44, pp. 111–118. DOI: <https://doi.org/10.1016/j.jsr.2012.08.020>.
- Kim, H., Ahn, C. R., and Yang, K. (2016) Identifying Safety Hazards Using Collective Bodily Responses of Workers, *Journal of Construction Engineering and Management*, Vol. 143, No. 2, pp. 04016090. DOI: [https://doi.org/10.1061/\(ASCE\)CO.1943-7862.0001220](https://doi.org/10.1061/(ASCE)CO.1943-7862.0001220).
- Kim, H., Ahn, C. R., Stentz, T. L., and Jebelli, H. (2018) Assessing the Effects of Slippery Steel Beam Coatings to Ironworkers' Gait Stability, *Applied Ergonomics*, Vol. 68, pp. 72–79. DOI: <https://doi.org/10.1016/j.apergo.2017.11.003>.
- Kong, L., Li, H., Yu, Y., Luo, H., Skitmore, M., and Antwi-Afari, M. F. (2018) Quantifying the Physical Intensity of Construction Workers, a Mechanical Energy Approach, *Advanced Engineering Informatics*, Vol. 38, pp. 404–419. DOI: <https://doi.org/10.1016/j.aei.2018.08.005>.
- Lee, H., Lee, K., and Park, M. (2011) RFID-based Real-Time Locating System for Construction Safety Management, *Journal of Computing in Civil Engineering*, Vol. 26, No. 3, pp. 366–377. DOI: [https://doi.org/10.1061/\(ASCE\)CP.1943-5487.0000144](https://doi.org/10.1061/(ASCE)CP.1943-5487.0000144).
- Li, G., Liu, T., and Yi, J. (2018) Wearable Sensor System for Detecting Gait Parameters of Abnormal Gaits: A Feasibility Study. *IEEE Sensors Journal*, Vol. 18, No. 10, pp. 4234–4241. DOI: <https://doi.org/10.1109/JSEN.2018.2814994>.
- Lin, F., Wang, A., Zhuang, Y., Tomita, M. R., and Xu, W. (2016) Smart Insole: A Wearable Sensor Device for Unobtrusive Gait Monitoring in Daily Life, *IEEE Transactions on Industrial Informatics*, Vol. 12, No. 6, pp. 2281–2291. DOI: <https://doi.org/10.1109/TII.2016.2585643>.
- Mitropoulos, P., and Namboodiri, M. (2011) New Method for Measuring the Safety Risk of Construction Activities: Task Demand Assessment, *Journal of Construction Engineering and Management*, Vol. 137, No. 1, pp. 30–38. DOI: [https://doi.org/10.1061/\(ASCE\)CO.1943-7862.0000246](https://doi.org/10.1061/(ASCE)CO.1943-7862.0000246).
- Muniz, A. M. S., and Nadal, J. (2009) Application of Principal Component Analysis in Vertical Ground Reaction Force to Discriminate Normal and Abnormal Gait, *Gait & Posture*, Vol. 29, No. 1, pp. 31–35. DOI: <https://doi.org/10.1016/j.gaitpost.2008.05.015>.
- Nsenga Leunkeu, A., Lelard, T., Shephard, R. J., Doutrelot, P. L., and Ahmaidi, S. (2014) Gait Cycle and Plantar Pressure Distribution in Children with Cerebral Palsy: Clinically Useful Outcome Measures for a Management and Rehabilitation, *NeuroRehabilitation*, Vol. 35, No. 4, pp. 657–663. DOI: <https://doi.org/10.3233/NRE-141163>.
- O'Sullivan, S. B., Schmitz, T. J., and Fulk, G. (2019) *Physical Rehabilitation*, 7th Edition, Philadelphia, PA: FA Davis. ISBN: 9780803694644.
- Park, J., Kim, K., and Cho, Y. K. (2016) Framework of Automated Construction-Safety Monitoring Using Cloud-Enabled BIM and BLE Mobile Tracking Sensors, *Journal of Construction Engineering and Management*, Vol. 143, No. 2, pp. 05016019. DOI: [https://doi.org/10.1061/\(ASCE\)CO.1943-7862.0001223](https://doi.org/10.1061/(ASCE)CO.1943-7862.0001223).
- Park, J., Marks, E., Cho, Y. K., and Suryanto, W. (2015) Performance Test of Wireless Technologies for Personnel and Equipment Proximity Sensing in Work Zones, *Journal of Construction Engineering and Management*, Vol. 142, No. 1, pp. 04015049. DOI: [https://doi.org/10.1061/\(ASCE\)CO.1943-7862.0001031](https://doi.org/10.1061/(ASCE)CO.1943-7862.0001031).
- Qi, J., Issa, R. R., Olbina, S., and Hinze, J. (2013) Use of Building Information Modeling in Design to Prevent Construction Worker Falls, *Journal of Computing in Civil Engineering*, Vol. 28, No. 5, pp. A4014008. DOI: [https://doi.org/10.1061/\(ASCE\)CP.1943-5487.0000365](https://doi.org/10.1061/(ASCE)CP.1943-5487.0000365).
- Rozenfeld, O., Sacks, R., Rosenfeld, Y., and Baum, H. (2010) Construction Job Safety Analysis, *Safety Science*, Vol. 48, No. 4, pp. 491–498. DOI: <https://doi.org/10.1016/j.ssci.2009.12.017>.
- Safe Work Australia (2017) *Key Work Health and Safety Statistics Australia 2017: Work-Related Injury Fatalities*. Available at: https://www.safeworkaustralia.gov.au/system/files/documents/1709/em17-0212_swa_key_statistics_overview_0.pdf (Accessed: October 2019).
- Schepers, H. M., Koopman, H. F., and Veltink, P. H. (2007) Ambulatory Assessment of Ankle and Foot Dynamics, *IEEE Transactions on Biomedical Engineering*, Vol. 54, No. 5, pp. 895–902. DOI: <https://doi.org/10.1109/TBME.2006.889769>.

- Scott-Pandorf, M. M., Stergiou, N., Johanning, J. M., Robinson, L., Lynch, T. G., and Pipinos, I. I. (2007) Peripheral Arterial Disease Affects Ground Reaction Forces During Walking, *Journal of Vascular Surgery*, Vol. 46, No. 3, pp. 491-499. DOI: <https://doi.org/10.1016/j.jvs.2007.05.029>.
- Solanki, D. S., and Lahiri, U. (2018) Design of Instrumented Shoes for Gait Characterization: A Usability Study with Healthy and Post-Stroke Hemiplegic Individuals, *Frontiers in Neuroscience*, Vol. 12, pp. 459. DOI: <https://doi.org/10.3389/fnins.2018.00459>.
- Teizer, J., Allread, B. S., Fullerton, C. E., and Hinze, J. (2010) Autonomous Pro-Active Real-Time Construction Worker and Equipment Operator Proximity Safety Alert System, *Automation in Construction*, Vol. 19, No. 5, pp. 630–640. DOI: <http://dx.doi.org/10.1016/j.autcon.2010.02.009>.
- Umer, W., Antwi-Afari, M. F., Li, H., Szeto, G. P. Y., and Wong, A. Y. L. (2017a) The Global Prevalence of Musculoskeletal Disorders in the Construction Industry: A Systematic Review and Meta-Analysis, *International Archives of Occupational and Environmental Health*, pp. 1–20. DOI: <https://doi.org/10.1007/s00420-017-1273-4>.
- Valero, E., Sivanathan, A., Bosché, F., and Abdel-Wahab, M. (2017) Analysis of Construction Trade Worker Body Motions Using a Wearable and Wireless Motion Sensor Network, *Automation in Construction*, Vol. 83, pp. 48-55. DOI: <https://doi.org/10.1016/j.autcon.2017.08.001>.
- Wang, J., and Razavi, S. N. (2016) Low False Alarm Rate Model for Unsafe-Proximity Detection in Construction, *Journal of Computing in Civil Engineering*, Vol. 30, No. 2, pp. 1–13. DOI: [http://dx.doi.org/10.1061/\(ASCE\)CP.1943-5487.0000470](http://dx.doi.org/10.1061/(ASCE)CP.1943-5487.0000470).
- Weerasinghe, I. T., Ruwanpura, J. Y., Boyd, J. E., and Habib, A. F. (2012). Application of Microsoft Kinect sensor for tracking construction workers, *Proceedings of ASCE Construction Research Congress*, West Lafayette, Indiana, May 21-23, 2012, pp. 858-867. DOI: <https://doi.org/10.1061/9780784412329.087>.
- Wong, L., Wang, Y., Law, T., and Lo, C. T. (2016) Association of Root Causes in Fatal Fall-From Height Construction Accidents in Hong Kong, *Journal of Construction Engineering and Management*, Vol. 142, No. 7, pp. 04016018. DOI: [https://doi.org/10.1061/\(ASCE\)CO.1943-7862.0001098](https://doi.org/10.1061/(ASCE)CO.1943-7862.0001098).
- Wren, T. A., Do, K. P., Hara, R., Dorey, F. J., Kay, R. M., and Otsuka, N. Y. (2007) Gillette Gait Index as a Gait Analysis Summary Measure: Comparison with Qualitative Visual Assessments of Overall Gait, *Journal of Pediatric Orthopaedics*, Vol. 27, No. 7, pp. 765-768. DOI: <https://doi.org/10.1097/BPO.0b013e3181558ade>.
- Yang, K., Ahn, C. R., and Kim, H. (2018) Tracking Divergence in Workers' Trajectory Patterns for Hazard Sensing in Construction, *Construction Research Congress*, New Orleans, Louisiana, April 2-4, 2018, pp.126–133. DOI: <https://doi.org/10.1061/9780784481288.013>.
- Yang, K., Ahn, C. R., and Kim, H. (2019) Validating Ambulatory Gait Assessment Technique for Hazard Sensing in Construction Environments, *Automation in Construction*, Vol. 98, pp. 302-309. DOI: <https://doi.org/10.1016/j.autcon.2018.09.017>.
- Yang, K., Ahn, C. R., Vuran, M. C., and Aria, S. S. (2016) Semi-Supervised Near-Miss Fall Detection for Ironworkers with A Wearable Inertial Measurement Unit, *Automation in Construction*, Vol. 68, pp. 194–202. DOI: <http://dx.doi.org/10.1016/j.autcon.2016.04.007>.
- Yang, K., Ahn, C. R., Vuran, M. C., and Kim, H. (2017) Collective Sensing of Workers' Gait Patterns to Identify Fall Hazards in Construction, *Automation in Construction*, Vol. 82, pp. 166-178. DOI: <https://doi.org/10.1016/j.autcon.2017.04.010>.
- Yang, K., and Ahn, C. R. (2019) Inferring Workplace Safety Hazards from the Spatial Patterns of Workers' Wearable Data, *Advanced Engineering Informatics*, Vol. 41, pp. 100924. DOI: <https://doi.org/10.1016/j.aei.2019.100924>.
- Yoon, H. Y., and Lockhart, T. E. (2006) Non-fatal Occupational Injuries Associated with Slips and Falls in The United States, *International Journal of Industrial Ergonomics*, Vol. 36, pp. 83–92. DOI: <https://doi.org/10.1016/j.ergon.2005.08.005>.